

Massive Neutrinos in Astrophysics

Lectures at the fourth national summer school
“Grundlagen und neue Methoden der theoretischen Physik”
31 August – 11 September 1998, Saalburg, Germany

Georg G. Raffelt

*Max-Planck-Institut für Physik
(Werner-Heisenberg-Institut)
Föhringer Ring 6, 80805 München, Germany
Email: raffelt@mppmu.mpg.de*

Lecture notes written by

Werner Rodejohann

*Lehrstuhl Theoretische Physik III
Universität Dortmund
Otto-Hahn Str. 4, 44221 Dortmund, Germany
Email: rodejoha@dilbert.physik.uni-dortmund.de*

ABSTRACT

An introduction to various topics in neutrino astrophysics is given for students with little prior exposure to this field. We explain neutrino production and propagation in stars, neutrino oscillations, and experimental searches for this effect. We also touch upon the cosmological role of neutrinos. A number of exercises is also included.

Contents

Table of Contents	i
Preface	iii
1 Neutrinos in Normal Stars	1
1.1 The Sun	1
1.2 Photon Dispersion in Stellar Plasmas	3
1.3 Neutrino Refraction in Media	4
1.4 Exercises	6
1.4.1 Constraints on Neutrino Dipole Moments	6
1.4.2 Supernova Neutrinos and Refraction	8
1.4.3 Neutrino Refraction in the Early Universe	8
1.4.4 The Sun as a Neutrino Lens	9
2 Neutrino Oscillations	11
2.1 Vacuum Oscillations	11
2.2 Oscillation in Matter	13
2.2.1 Homogeneous Medium	13
2.2.2 MSW Effect	16
2.3 Exercises	17
2.3.1 Polarization vector and neutrino oscillations	17
2.3.2 MSW Effect in the Sun	18
3 Experimental Oscillation Searches	20
3.1 Typical Scales	20
3.2 Atmospheric neutrino experiments	20
3.3 Accelerator Experiments	22
3.4 Reactor Experiments	22
3.5 Solar Neutrino Experiments	23
3.6 Summary of Experimental Results	25
4 Neutrinos in Cosmology	27
4.1 Friedmann Equation and Cosmological Basics	27
4.2 Radiation Epoch	29
4.3 Present-Day Neutrino Density	30
4.4 Big Bang Nucleosynthesis	32
4.5 Neutrinos as Dark Matter	36

5	Conclusions	39
A	Useful Tables	40
A.1	Integrals	40
A.2	Conversion of Units	40
	References	41

Preface

Neutrino astrophysics is a prime example for the modern connection between astrophysics and particle physics which is often referred to as “astroparticle physics” or also “particle astrophysics.” The intrinsic properties of neutrinos, especially the question of their mass, is one of the unsolved problems of particle physics. On the other hand, neutrino masses and other more hypothetical properties such as electromagnetic couplings can play an important role in various astrophysical environments. Therefore, astrophysics plays an important role at constraining nonstandard neutrino properties.

Of course, the most exciting recent development is the overwhelming evidence for neutrino oscillations from the atmospheric neutrino anomaly, and notably the zenith–angle variation observed in the SuperKamiokande experiment. Besides the near–certainty that the phenomenon of neutrino oscillations is real, this high–statistics experiment has also opened a new era in neutrino astronomy. It may not be too long until large–scale neutrino telescopes observe novel astrophysical sources in the “light” of neutrino radiation.

In these lectures we cover a number of topics in the area of neutrino astrophysics and cosmology which are of current interest to an audience of students who have not had much prior exposure to either neutrino physics, astrophysics, or cosmology. At the summer school, the lectures were presented on a chalk board, with only a small number of viewgraph projections, severely limiting the amount of material that could be covered in a few hours. Some of the material was treated in two exercise sessions; some of the exercises are integrated into the present notes. Still, these lectures are rather incomplete and give only a first impression of the field.

For a more complete coverage the reader is referred to the excellent textbook by Schmitz [1], which unfortunately is available only in German. Many of the stellar–evolution topics are covered in “Stars as Laboratories for Fundamental Physics” by Raffelt [2]. For the cosmological questions, the best textbook reference remains the classic by Kolb and Turner [3]. A good overview of many of the relevant issues is provided in two recent textbooks on astroparticle physics [4, 5]. Finally, we mention a few recent review articles which may be of help to access the field in more depth [6, 7, 8, 9].

Chapter 1 treats the production of neutrinos in normal stars, especially in the Sun, but leaving out supernova physics —there simply was not enough time to treat this complicated topic in the lectures. Chapter 2 discusses neutrino oscillations in vacuum and in matter. In Chapter 3, experimental strategies are reviewed and some experiments are described in more detail. Chapter 4 is devoted to the connection of neutrinos and cosmology. Conclusions are presented in Chapter 5.

1 Neutrinos in Normal Stars

1.1 The Sun

Ever since it became clear that stars are powered by nuclear fusion reactions and that neutrinos are produced in nuclear reactions, it was also clear that stars are powerful neutrino sources. Stellar evolution proceeds through many distinct evolutionary phases [10, 11]. Stars spend most of their lives on the initial “main–sequence,” the Sun is an example, where energy is gained from the fusion of hydrogen to helium, i.e. by the net reaction



The detailed reaction chains and cycles depend on the stellar mass which, in turn, influences the equilibrium temperature in the interior. In the case of a low–mass star like the Sun, hydrogen burning proceeds primarily through the pp chains. The CNO cycle (Bethe–Weizsäcker cycle), which dominates in more massive stars, contributes only about 1.6%.

From the particle physics perspective, the solar neutrino flux is perhaps the most important example because it has been measured in several different experiments, giving rise to the “solar neutrino problem” and thus provides evidence for neutrino oscillations. From Eq. (1) one sees that two electron neutrinos are produced for every 26.7 MeV of liberated nuclear energy. Assuming that the neutrinos themselves carry away only a small fraction of this energy, the total solar flux at Earth can be estimated as

$$\Phi_{\nu_e} \simeq 2 \frac{S}{26.7 \text{ MeV}} = 2 \frac{8.5 \times 10^{11} \text{ MeV cm}^{-2} \text{ s}^{-1}}{26.7 \text{ MeV}} = 6.4 \times 10^{10} \text{ cm}^{-2} \text{ s}^{-1}, \quad (2)$$

where S is the solar constant.

However, for the interpretation of the experiments, the detailed spectral characteristics of the solar neutrino flux are of great importance. In the pp chains, electron neutrinos are

Table 1: Solar neutrino production in the pp chains.

Name	Reaction	$\langle E_\nu \rangle$ [MeV]	E_ν^{max} [MeV]	Fractional solar flux
pp	$p + p \rightarrow \text{D} + e^+ + \nu_e$	0.26	0.42	0.909
pep	$p + e^- + p \rightarrow \text{D} + \nu_e$	1.44	—	2×10^{-3}
hep	${}^3\text{He} + p \rightarrow {}^4\text{He} + e^+ + \nu_e$	9.62	18.77	2×10^{-8}
${}^7\text{Be}$	${}^7\text{Be} + e^- \rightarrow {}^7\text{Li} + \nu_e$	(90%) 0.86 (10%) 0.38	—	0.074
${}^8\text{B}$	${}^8\text{B} \rightarrow {}^8\text{Be}^* + e^+ + \nu_e$	6.71	≈ 15	8.6×10^{-5}

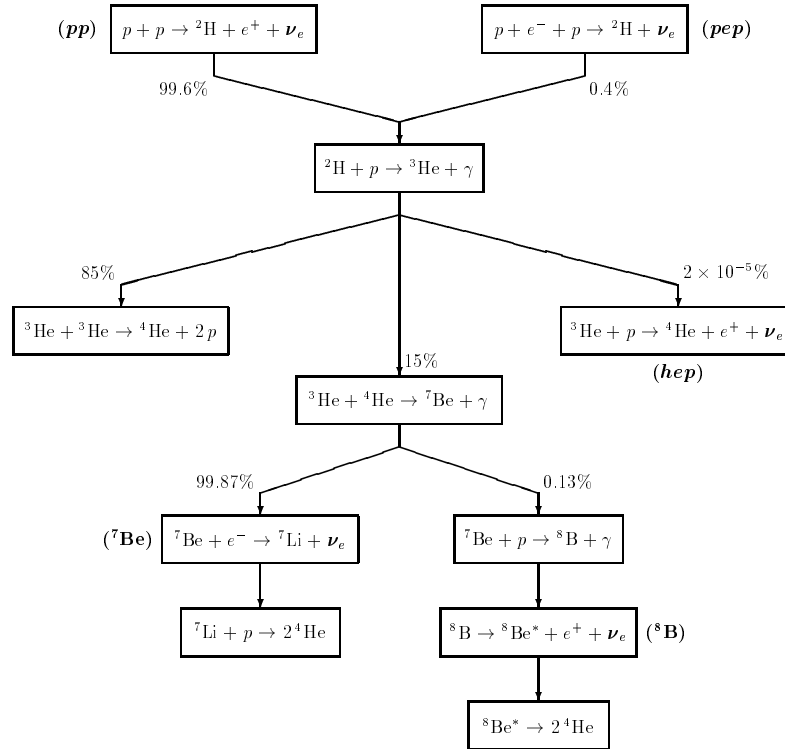


Figure 1: Energy generation in the Sun via the pp chains. (Figure from Ref. [9].)

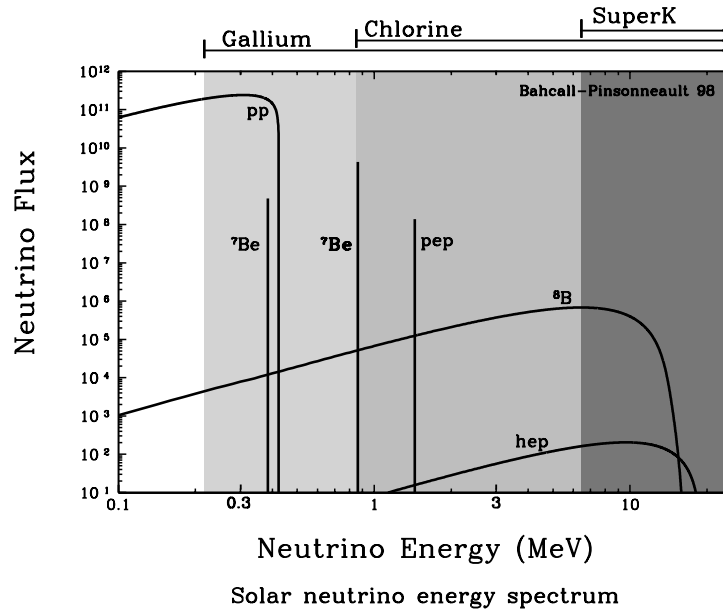


Figure 2: Solar neutrino spectrum and thresholds of solar neutrino experiments as indicated above the figure (taken from <http://www.sns.ias.edu/~jnb/>).

produced in six different reactions, giving rise to as many different spectral contributions (Table 1, Figs. 1 and 2), i.e. three monochromatic lines from electron capture reactions and three continuous beta-spectra. The sum of the fractional solar neutrino fluxes in Table 1 is less than unity due to the small CNO contribution.

The detailed contribution of each reaction is based on a standard solar model (SSM) [12] which describes the Sun on the basis of a well-defined set of input assumptions. There is broad consensus in the literature on the properties of a SSM. However, if the real Sun is indeed well represented by a SSM is not a trivial question. The enormous recent progress in the field of helioseismology, however, appears to confirm many detailed properties of the SSM. One measures the frequencies of the solar pressure modes (p modes) by the Doppler shift of spectral lines. One thus probes indirectly the speed of sound in the Sun at various depths, i.e. one can reconstruct a sound-speed profile of the Sun which is extremely sensitive to the temperature, density and composition profile.

1.2 Photon Dispersion in Stellar Plasmas

The nuclear reactions discussed thus far produce electron neutrinos in beta reactions where a ν_e appears together with an e^+ or at the expense of the absorption of an e^- . However, stellar plasmas emit neutrinos also by a variety of processes where $\nu\bar{\nu}$ pairs of all flavors appear by effective neutral-current reactions. The most important cases are

$$\begin{array}{ll}
 \text{Photo Process} & \gamma + e^- \rightarrow e^- + \nu + \bar{\nu}, \\
 \text{Pair Annihilation} & e^+ + e^- \rightarrow \nu + \bar{\nu}, \\
 \text{Bremsstrahlung} & e^- + (A, Z) \rightarrow (A, Z) + e^- + \nu + \bar{\nu}, \\
 \text{Plasma Process} & \gamma \rightarrow \nu + \bar{\nu}.
 \end{array} \tag{3}$$

The relative importance of these processes depends on the temperature and density of the plasma. The energy of the neutrinos produced in these reactions is of the order of the temperature of the plasma, in contrast with the nuclear reactions where the neutrino energy is determined by nuclear binding energies. In the Sun, the central temperature is about 1.3 keV so that thermal neutrino energies are much smaller than those produced in the pp chains. The total energy emitted by these processes in the Sun is negligibly small.

However, in later evolutionary phases, neutrinos produced by plasma processes become much more important than nuclear processes. In particular, the plasma process (“photon decay”) is the dominant neutrino-producing reaction in white dwarfs or the cores of horizontal-branch stars or low-mass red giants. This process is noteworthy because it is not possible in vacuum due to energy-momentum conservation. In a plasma, on the other

hand, the photon acquires a nontrivial dispersion relation (“effective mass”) so that its decay into neutrinos is kinematically possible.

We will see that medium-induced modifications of particle dispersion relations are not only important for the plasma process, but also for neutrino oscillations in the Sun or in other environments. One usually defines a refractive index n_{refr} which relates wave number and frequency of a particle by $k = n_{\text{refr}}\omega$. Refraction in a medium arises from the interference of the incoming wave with the scattered waves in the forward direction. Therefore, the refractive index is given in terms of the forward-scattering amplitude f_0 by

$$n_{\text{refr}} = 1 + \frac{2\pi}{\omega^2} n f_0(\omega), \quad (4)$$

where n is the number density of the scattering targets. This formula applies to any particle propagating in a medium, except that f_0 must be calculated according to the interactions of that particle with the medium constituents.

Photons interact electromagnetically; the dominant scattering process is Compton scattering on electrons $\gamma + e^- \rightarrow e^- + \gamma$. In the low-energy limit (Thomson scattering) one finds $f_0 = -\alpha/m_e$ with $\alpha = 1/137$ the fine-structure constant. It is then trivial to show that the refractive index corresponds to a dispersion relation

$$\omega^2 - k^2 = \omega_p^2 = \frac{4\pi\alpha}{m_e} n_e, \quad (5)$$

where ω_p is the so-called plasma frequency. In the Sun, for example, one finds $\omega_p \simeq 0.3$ keV while in the core of low-mass red giants it is about 9 keV (Exercise 1.4.1). The plasma frequency plays the role of an effective photon mass. We stress, however, that the general photon dispersion relation or that of other particles can not be written in this simple form, i.e. in general the effect of dispersion can not be represented by an effective in-medium mass.

1.3 Neutrino Refraction in Media

We next turn to the neutrino dispersion relation in media. Usually we will be concerned with very low energies. Therefore, we may take the low-energy limit of the weak-interaction Hamiltonian where the propagators for the massive gauge bosons are expanded as

$$D_{\mu\nu} = \frac{g_{\mu\nu}}{Q^2 - M_{W,Z}^2} \simeq \frac{-g_{\mu\nu}}{M_{W,Z}^2}. \quad (6)$$

In this limit one obtains the usual current-current Hamiltonian for the neutrino-fermion interaction,

$$\mathcal{H}_{\text{int}} = \frac{G_F}{\sqrt{2}} \bar{\psi}_f \gamma_\mu (C_V - C_A \gamma_5) \psi_{f'} \bar{\psi}_\nu \gamma^\mu (1 - \gamma_5) \psi_\nu, \quad (7)$$

where G_F is the Fermi constant.

One may then proceed to calculate the dispersion relation in a medium on the basis of Eq. (4). However, in the special case of a current–current interaction the neutrino energy shift in a medium can be calculated in a much simpler way. To this end we evaluate the expectation value of the current of the background fermions, $\langle \bar{\psi}_f \gamma_\mu (C_V - C_A \gamma_5) \psi_f \rangle$. The axial part (the term proportional to C_A) vanishes if the medium is unpolarized so that there is no preferred spin direction. The vector part is equivalent to $(n_f - n_{\bar{f}})u_\mu$ where n_f and $n_{\bar{f}}$ are the particle and antiparticle densities, respectively, and u is the medium’s four-velocity. Furthermore, we are only concerned with left-handed neutrino fields for which $\gamma_5 \psi_\nu = -\psi_\nu$ or $(1 - \gamma_5)\psi_\nu = 2\psi_\nu$. In summary, the interaction Hamiltonian of Eq. (7) amounts to

$$\sqrt{2}G_F C_V (n_f - n_{\bar{f}})u_\mu \bar{\psi}_\nu \gamma^\mu \psi_\nu. \quad (8)$$

In the rest frame of the medium we have no preferred direction (no bulk flows) so that $u = (1, 0, 0, 0)$. Therefore, a left-handed neutrino in a background medium feels a weak–interaction potential

$$V = \pm \sqrt{2}G_F C'_V (n_f - n_{\bar{f}}), \quad (9)$$

where the lower sign refers to anti-neutrinos. The dispersion relation is

$$\omega = V + k, \quad (10)$$

which evidently does not resemble the one for a massive particle. Therefore, one can not define an “effective neutrino mass” in the medium.

The relevant coupling constants C'_V for various background particles are given in Table 2. For most cases, C'_V is identical with the neutral–current coupling C_V . However, if f is the charged lepton belonging to the neutrino, an additional term with $C_V = 1$ from the Fierz–transformed charged current occurs. For $f = \nu$ we have a factor 2 for the exchange amplitude of two identical particles.

In an electrically neutral, normal medium we have as many protons as electrons, at least if the temperature is low enough that muons and pions are not present, so that

$$V = \pm \sqrt{2}G_F \times \begin{cases} -\frac{1}{2}n_n + n_e & \text{for } \nu_e, \\ -\frac{1}{2}n_n & \text{for } \nu_\mu \text{ and } \nu_\tau. \end{cases} \quad (11)$$

The plus sign is for neutrinos, the minus sign for antineutrinos. For $n_e < \frac{1}{2}n_n$ (e.g. in a neutron star) the potential produced by the medium is negative for neutrinos and positive for antineutrinos. It is important to note that the extra contribution for the electron flavor stems from the charged–current interaction in $\nu_e + e \rightarrow \nu_e + e$, which is not possible for the other flavors.

Table 2: Effective coupling constants for refraction of neutrinos in a medium of background fermions. Note that $\sin^2 \Theta_W = 0.226$.

Fermion f	Neutrino	C'_V
Electron	ν_e	$+\frac{1}{2} + 2 \sin^2 \Theta_W$
	ν_μ, ν_τ	$-\frac{1}{2} + 2 \sin^2 \Theta_W$
Proton	ν_e, ν_μ, ν_τ	$+\frac{1}{2} - 2 \sin^2 \Theta_W$
Neutron	ν_e, ν_μ, ν_τ	$-\frac{1}{2}$
Neutrino ν_a	ν_a	$+1$
	$\nu_{b \neq a}$	$+\frac{1}{2}$

1.4 Exercises

1.4.1 Constraints on Neutrino Dipole Moments

Neutrinos may have anomalous electric and magnetic dipole and transition moments, which are small in the standard model but can be large in certain extensions so that they have to be constrained. The Lagrangian is

$$\mathcal{L}_{\text{int}} = \frac{1}{2} \sum_{a,b} \left(\mu_{ab} \bar{\psi}_a \sigma_{\mu\nu} \psi_b + \epsilon_{ab} \bar{\psi}_a \sigma_{\mu\nu} \gamma_5 \psi_b \right) F^{\mu\nu}, \quad (12)$$

where the indices a and b run over the neutrino families, μ_{ab} is a magnetic, ϵ_{ab} an electric transition moment, respectively, and a static magnetic or electric dipole moment for $a = b$. (Note that electric dipole moments are CP violating.) These moments are measured in units of the Bohr magneton $\mu_B = e/2m_e$. $F^{\mu\nu}$ is the electromagnetic field tensor and $\sigma_{\mu\nu} = \frac{i}{2}(\gamma_\mu \gamma_\nu - \gamma_\nu \gamma_\mu)$.

- Calculate the decay width $\gamma \rightarrow \nu \bar{\nu}$ for a neutrino family with a magnetic dipole moment μ , when photons have an effective mass ω_p , as seen in Eq. (5).
- Calculate the energy loss rate in neutrinos of a nonrelativistic plasma at the temperature T .
- The cores of low-mass red giant stars (about $0.5 M_\odot$, solar mass $M_\odot = 2 \times 10^{33}$ g) have an average density of approximately 2×10^5 g cm $^{-3}$ and are almost isothermal at 10^8 K. In order not to delay helium ignition too much, the neutrino loss rate ϵ is not allowed to exceed about 10 erg g $^{-1}$ s $^{-1}$. Which limit is obtained for μ ?

- d) This limit is also valid for transition moments, which can lead to decays like $\nu_2 \rightarrow \nu_1 + \gamma$. Why does the direct search for these radiative decays of massive neutrinos make no sense, provided one believes in the bound for μ obtained above?
- e) Estimate or calculate a similar bound for a hypothetical electric charge (millicharge) of a neutrino.

Hints

Work in the rest frame of the medium. Show that the squared and spin summed matrix element is of the form

$$|\mathcal{M}|^2 = M_{\alpha\beta} P^\alpha \bar{P}^\beta, \quad (13)$$

where P and \bar{P} are the four-momenta of the neutrino and antineutrino, respectively, and

$$M_{\alpha\beta} = 4\mu^2 \left(2K_\alpha K_\beta - 2K^2 \epsilon_\alpha^* \epsilon_\beta - K^2 g_{\alpha\beta} \right), \quad (14)$$

where $K = (\omega, \mathbf{k})$ is the photon four momentum and ϵ its polarization four vector. We have $\epsilon_\alpha^* \epsilon^\alpha = -1$ and $\epsilon_\alpha K^\alpha = 0$. For the neutrino phase-space integration use Lenard's formula

$$\int \frac{d^3\mathbf{p}}{2E_{\mathbf{p}}} \frac{d^3\bar{\mathbf{p}}}{2E_{\bar{\mathbf{p}}}} P^\alpha \bar{P}^\beta \delta(K - P - \bar{P}) = \frac{\pi}{24} (K^2 g^{\alpha\beta} + 2K^\alpha K^\beta). \quad (15)$$

The decay width is finally found to be

$$\Gamma_{\gamma \rightarrow \nu\bar{\nu}} = \frac{\mu^2}{24\pi} \frac{(\omega^2 - k^2)^2}{\omega}. \quad (16)$$

Note that the decay would be impossible in vacuum where $\omega = k$. In the present situation, however, we may insert the dispersion relation $\omega^2 - k^2 = \omega_{\mathbf{p}}^2$ to obtain the decay rate.

Since every photon decay liberates the energy ω in the form of neutrinos, the energy-loss rate per unit volume is

$$Q = g \int \frac{d^3k}{(2\pi)^3} f_k \omega \Gamma_{\gamma \rightarrow \nu\bar{\nu}}, \quad (17)$$

with the photon distribution function f_k (Bose-Einstein) and $g = 2$ the number of polarization states. Useful integrals for this exercise are given in Table A.1.

The matrix element and the width for the radiative neutrino decay $\nu_2 \rightarrow \nu_1 + \gamma$ (transition dipole moment μ_{12}) are

$$|\mathcal{M}|^2 = 8\mu_{12}^2 (K \cdot P_1)(K \cdot P_2), \quad (18)$$

$$\Gamma_{\nu_2 \rightarrow \nu_1 + \gamma} = \frac{\mu_{12}^2}{8\pi} \left(\frac{m_2^2 - m_1^2}{m_2} \right)^3,$$

where P_i denotes the momentum of neutrino ν_i with mass m_i and K the photon momentum.

1.4.2 Supernova Neutrinos and Refraction

A type II supernova explosion is actually the implosion of the burnt-out iron core (mass around $1.4 M_\odot$) of a massive star. This collapse leads to a compact object with nuclear density ($3 \times 10^{14} \text{ g cm}^{-3}$) and a radius of about 12 km.

- a) What is the gravitational binding energy?
- b) 99% of this energy is emitted in ν 's and $\bar{\nu}$'s of all flavors. When the time for this process is 10 s, what is the luminosity (in erg s^{-1}) in one neutrino degree of freedom?
- c) The average energy of the emitted neutrinos is

$$\langle E_\nu \rangle = \begin{cases} 10 \text{ MeV} & \text{for } \nu_e, \\ 14 \text{ MeV} & \text{for } \bar{\nu}_e, \\ 20 \text{ MeV} & \text{other.} \end{cases} \quad (19)$$

What is the number flux at the time of emission? What is the local neutrino density (per flavor) as a function of the radius above the neutron star surface?

- d) At the surface of the neutron star the matter density falls off steeply. Assume that it follows a power law $\rho = \rho_R(R/r)^p$ with $p = 3 - 7$ and $\rho_R = 10^{14} \text{ g cm}^{-3}$. How does the electron density compare with the neutrino density during their emission? Assume that the medium has as many protons as neutrons.
- e) Compare the weak potential produced by the neutrinos with the one produced by normal matter. Assume that the energy flux is the same in all flavors, but the average energy is not, see Eq. (19). Therefore, only for the electron flavor a difference between particles and antiparticles exists and thus a net contribution to the weak potential. Another important point is that the ν 's are emitted almost collinear so that the background medium of neutrinos is not isotropic relative to a test neutrino; for an exactly pointlike source there would be no contribution at all.

1.4.3 Neutrino Refraction in the Early Universe

The “normal” neutrino refractive index is calculated on the basis of the Fermi interaction (current–current interaction). It can be interpreted as a weak potential for the neutrinos. The medium in the early universe is almost CP–invariant —all particles have almost the same number density as their antiparticles. Thus the refractive index nearly cancels to this order. A weak potential arises only from the matter–antimatter asymmetry of $\eta \simeq 3 \times 10^{-10}$ baryons per photon.

- a) Using this value for η , estimate the “normal” refractive index of neutrinos in the radiation dominated era before e^+e^- annihilation. Use dimensional arguments to express n_{refr} as a function of the cosmic temperature T . (Hint: the number density of relativistic thermal particles is proportional to T^3 .)
- b) Which Feynman diagrams contribute to neutrino forward scattering and thus to the refractive index?
- c) The gauge boson propagator can be expanded if the momentum transfer Q is small relative to the gauge boson mass,

$$D_{\mu\nu} = \frac{g_{\mu\nu}}{M_{Z,W}^2} + \frac{Q^2 g_{\mu\nu} - Q_\mu Q_\nu}{M_{Z,W}^4} + \dots \quad (20)$$

The first term provides the Fermi theory of weak interactions. For which diagram is the current–current term the exact result? For which diagrams does one have to take higher terms into account?

- d) Can you imagine other corrections which might be as important as the propagator expansion?
- e) Estimate, again in form of a dimensional analysis, the contribution of the higher terms in the early universe. Compare with a). Interpretation?

Remark

If the medium consists of neutrinos of all flavors and of e^+e^- , an exact calculation for the CP asymmetric contribution in the early universe gives $n_{\text{refr}} - 1 = \xi G_F^2 T^4 / \alpha$ with $\xi = \frac{14}{45}\pi(3 - \sin^2 \Theta_W) \sin^2 \Theta_W \simeq 0.61$ for ν_e or $\bar{\nu}_e$, while for the other flavors one finds $\xi = \frac{14}{45}\pi(1 - \sin^2 \theta_W) \sin^2 \Theta_W \simeq 0.17$.

1.4.4 The Sun as a Neutrino Lens

The neutrino refractive index in media is important for oscillation phenomena. Can it be responsible for conventional refractive effects? Estimate the deflection angle of a neutrino beam when it hits a spherical body with a given impact parameter. Give a crude numerical value for the Sun. Compare with gravitational deflection.

Hints

Assume parallel layers of the medium and a beam which propagates at an angle α relative to the density gradient. The refraction law informs us that $n_{\text{refr}} \sin \alpha = \text{const}$, where n_{refr} is

the refractive index. Differentiating and some manipulations give for the beam deflection

$$\frac{d\alpha}{ds} = \frac{|\nabla_{\perp} n|}{n_{\text{refr}}}, \quad (21)$$

where s is a coordinate along the beam and ∇_{\perp} the gradient transverse to the local beam direction. Since $|n_{\text{refr}} - 1| \ll 1$ one can take $n_{\text{refr}} = 1$ in the denominator. The deflection is so small that to lowest order the beam travels on a straight line.

The neutrino refractive index is $n_{\text{refr}} = 1 - m_{\nu}^2/2E_{\nu}^2 - V/E$, where V is the weak potential of Eq. (11). Numerically one finds $\sqrt{2}G_F\rho/m_u = 0.762 \times 10^{-13} \text{ eV } \rho/(\text{g cm}^{-3})$ with the mass density ρ and the atomic mass unit m_u . The density at the center of the Sun is about 150 g cm^{-3} and the radius of the Sun is $R_{\odot} = 6.96 \times 10^{10} \text{ cm}$.

Gravitation affects the beam deflection through the “refractive index” $n_{\text{refr}} = 1 - 2\Phi$, where Φ is the gravitational potential. In natural units, Newton’s constant is $G_N = 1/m_{\text{Pl}}^2$ with the Planck mass $m_{\text{Pl}} = 1.22 \times 10^{19} \text{ GeV}$.

2 Neutrino Oscillations

2.1 Vacuum Oscillations

If neutrinos have nonzero masses — and thus have properties beyond the standard model — they can oscillate between the flavor eigenstates. A flavor eigenstate is operationally defined as a neutrino state which appears in association with a given charged lepton. For example, the anti-neutrino emerging from neutron decay $n \rightarrow p + e^- + \bar{\nu}_e$ is by definition an electron anti-neutrino. Likewise, the reaction $\mu^- + p \rightarrow n + \nu_\mu$ produces a muon neutrino. Within the standard model, flavor-changing neutral currents do not exist, i.e. in a scattering process of the form $\nu + n \rightarrow n + \nu$ the out-going neutrino has exactly the same flavor as the incoming one. However, in analogy to the quark sector, the flavor eigenstates need not be eigenstates of the mass operator. If neutrinos have masses at all, it is generally assumed that the mass operator violates the conservation of individual lepton-flavor numbers.

The simplest example is that of two lepton families. The mass eigenstates ν_j , $j = 1, 2$ are connected to the flavor eigenstates ν_α and ν_β via

$$\begin{pmatrix} \nu_\alpha \\ \nu_\beta \end{pmatrix} = \begin{pmatrix} \cos \theta & \sin \theta \\ -\sin \theta & \cos \theta \end{pmatrix} \begin{pmatrix} \nu_1 \\ \nu_2 \end{pmatrix}. \quad (22)$$

Depending on the context, ν_j may stand for the neutrino field operator or simply for a neutrino state, in which case ν_j stands for $|\nu_j\rangle$. The mixing matrix is unitary and therefore has one nontrivial free parameter, the mixing angle θ . For three (n) families, the mixing matrix would have three $[\frac{1}{2}n(n-1)]$ nontrivial angles θ_j . In addition, for Dirac neutrinos it has one $[\frac{1}{2}(n-2)(n-1)]$ CP-violating phase(s), and three $[\frac{1}{2}n(n-1)]$ nontrivial phases for Majorana neutrinos. However, it can be shown that in oscillation experiments only the number of phases given by the Dirac case, i.e. one $[\frac{1}{2}(n-2)(n-1)]$ can be measured. We have therefore the same structure as for the Cabbibo–Kobayashi–Maskawa (CKM) matrix in the quark sector of the standard model.

It is easy to see how neutrino oscillations arise if we imagine that a neutrino with energy E of a given flavor, for example ν_e , is produced at some location $\mathbf{x} = 0$. It can be decomposed into mass eigenstates according to Eq. (22) so that

$$\nu(0) = \nu_e = \cos \theta \nu_1 + \sin \theta \nu_2. \quad (23)$$

We imagine the mass eigenstates to propagate as plane waves so that each of them evolves along the beam as

$$\nu_j e^{-i(Et - \mathbf{p}_j \cdot \mathbf{x})} \quad (24)$$

with $j = 1$ or 2 . Here,

$$p_j = |\mathbf{p}_j| = (E^2 - m_j^2)^{1/2} \simeq E - \frac{m_j^2}{2E}, \quad (25)$$

where the last approximation holds in the relativistic limit $m_j \ll E$. This is surely justified since one expects m_j to be smaller than a few eV and typical energies start at a few MeV. Therefore, the original state of Eq. (23) evolves as

$$\nu(x) = e^{-iE(t-x)} \left(\cos \theta e^{i(m_1^2/2E)x} \nu_1 + \sin \theta e^{i(m_2^2/2E)x} \nu_2 \right), \quad (26)$$

where $x = |\mathbf{x}|$. Next, we can invert Eq. (22) to express the mass eigenstates in terms of the flavor eigenstates, and insert these expressions into Eq. (26). Assuming the other flavor is ν_μ , one then finds immediately that the ν_μ amplitude of the beam evolves as

$$\langle \nu_\mu | \nu_e \rangle = \frac{1}{2} \sin 2\theta \left(e^{i(m_2^2/2E)x} - e^{i(m_1^2/2E)x} \right) e^{-iE(t-x)}. \quad (27)$$

Squaring this amplitude gives us the probability for observing a ν_μ at a distance x from the production site

$$P(\nu_e \rightarrow \nu_\mu) = \sin^2 2\theta \sin^2 \left(\frac{x \delta m^2}{4E} \right), \quad (28)$$

where $\delta m^2 \equiv m_2^2 - m_1^2$. A mono-energetic neutrino beam thus oscillates with amplitude $\sin^2 2\theta$ and wave number $k_{\text{osc}} = \delta m^2/4E$ (Fig. 3). The maximum effect occurs for $\theta = \pi/4$. One usually defines the oscillation length

$$\ell_{\text{osc}} = \frac{4\pi E}{\delta m^2} = 2.48 \text{ m} \frac{E}{1 \text{ MeV}} \frac{1 \text{ eV}^2}{\delta m^2}. \quad (29)$$

The neutrino beam has returned to its original state after traveling a distance ℓ_{osc} . The probability for finding the neutrino in its original state after traveling a distance x is $P(\nu_e \rightarrow \nu_e) = 1 - P(\nu_e \rightarrow \nu_\mu)$.

Note that oscillations would be impossible for completely degenerate masses ($m_1^2 = m_2^2$), including the case of vanishing neutrino masses, or for a vanishing mixing angle.

The generalization of these results to three or more families is straightforward but complicated; it can be found in many textbooks, e.g. in Ref. [1]. Equation (28) then reads

$$P(\alpha \rightarrow \beta) = \delta_{\alpha\beta} - 2 \Re \sum_{j>i} U_{\alpha i} U_{\alpha j}^* U_{\beta i}^* U_{\beta j} \left[1 - \exp \left(-i \frac{\Delta_{ij}}{4E} x \right) \right] \quad (30)$$

with $\Delta_{ij} = m_i^2 - m_j^2$. In general $P(\alpha \rightarrow \beta) \neq P(\beta \rightarrow \alpha)$ due to the complex phase of the unitary mixing matrix U , offering a possibility to measure this phase. A convenient

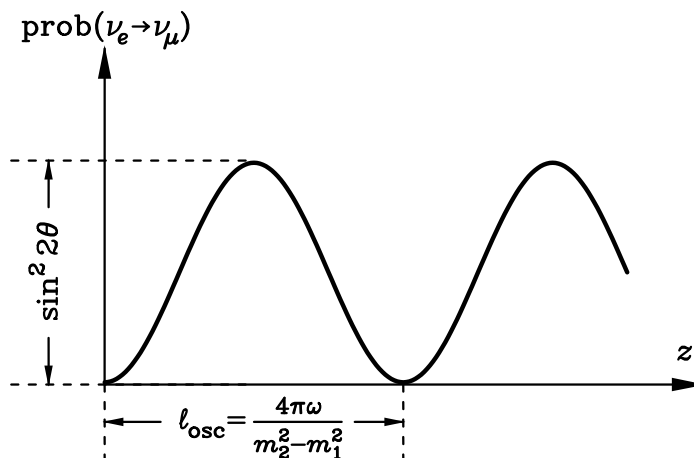


Figure 3: Oscillation pattern for two-flavor oscillations (neutrino energy ω , distance z).

parametrisation of U is

$$U = \begin{pmatrix} c_1 & s_1 c_3 & s_1 s_3 \\ -s_1 c_2 & c_1 c_2 c_3 - s_2 s_3 e^{i\delta} & c_1 c_2 s_3 + s_2 c_3 e^{i\delta} \\ s_1 s_2 & -c_1 s_2 c_3 - c_2 s_3 e^{i\delta} & -c_1 s_2 s_3 + c_2 c_3 e^{i\delta} \end{pmatrix} \quad (31)$$

with $s_i = \sin \theta_i$ and $c_i = \cos \theta_i$. For Majorana neutrinos U has to be multiplied with $\text{diag}(e^{i\lambda_1}, e^{i\lambda_2}, 1)$.

Thus far we have assumed that the neutrinos are mono-energetic and the sources and detectors are pointlike. Since nature is not so kind as to provide us with these simple cases, one has to convolute these formulas with energy and distance distributions. Naturally, these effects smear out the signature of oscillations, thereby complicating the interpretation of the experiments. A given experiment or observation usually provides exclusion or evidence regions in the parameter plane of $\sin^2 2\theta$ and δm^2 .

2.2 Oscillation in Matter

2.2.1 Homogeneous Medium

Neutrino oscillations arise over macroscopic distances because the momentum difference $\delta m^2/2E$ between two neutrino mass eigenstates of energy E is very small for neutrino masses in the eV range or below and for energies in the MeV range or above. Wolfenstein was the first to recognize that the neutrino refractive effect caused by the presence of a medium can cause a momentum difference of the same general magnitude, implying

that the extremely small weak potential for neutrinos in a medium can modify neutrino oscillations in observable ways.

In order to understand how the neutrino potential enters the oscillation problem, it is useful to back up and derive a more formal equation for the evolution of a neutrino beam. To this end we begin with the Klein–Gordon equation for the neutrino fields

$$(\partial_t^2 - \nabla^2 + M^2)\Psi = 0 \quad (32)$$

where in the general three-flavor case

$$M^2 = \begin{pmatrix} m_1^2 & 0 & 0 \\ 0 & m_2^2 & 0 \\ 0 & 0 & m_3^2 \end{pmatrix} \quad \text{and} \quad \Psi = \begin{pmatrix} \nu_1 \\ \nu_2 \\ \nu_3 \end{pmatrix}. \quad (33)$$

If we imagine neutrinos to be produced with a fixed energy E at some source, their wave functions vary as e^{-iEt} so that their spatial propagation is governed by the equation

$$(-E^2 - \partial_x^2 + M^2)\Psi = 0, \quad (34)$$

where we have reduced the spatial variation to one dimension, i.e. we consider plane waves.

In the relativistic limit $E \gg m_j^2$ we may linearize this wave equation by virtue of the decomposition $(-E^2 - \partial_x^2) = -(E + i\partial_x)(E - i\partial_x)$. Since $-i\partial_x \nu_j = p_j \nu_j$ with $p_j = (E^2 - m_j^2)^{1/2} \simeq E$ it is enough to keep the differential in the difference term, while replacing it with E in the sum, leading to $(-E^2 - \partial_x^2) \rightarrow -2E(E + i\partial_x)$. Therefore, in the relativistic limit the evolution along the beam is governed by a Schrödinger–type equation

$$i\partial_x \Psi = (-E + \Omega)\Psi, \quad \Omega = \frac{M^2}{2E}. \quad (35)$$

Usually this sort of equation is written down for the time–variation instead of the spatial one so that it looks more like a conventional Schrödinger equation. However, in the problem at hand we ask about the variation of the flavor content along a stationary beam, so that it is confusing to use a differential equation for the time variation which then has to be re–interpreted as describing the evolution along the beam. Either way, the main feature of this equation is that it is a complex linear equation involving a “Hamiltonian” matrix Ω ; the term $-E$ contributes a global phase which is irrelevant for the oscillation probability.

The potential caused by the medium is then easily included by adding it to the Hamiltonian

$$\Omega \rightarrow \Omega_M = \frac{M^2}{2E} + V \quad (36)$$

where V is a matrix of potentials which is diagonal in the weak–interaction basis with the entries given by Eq. (11).

As a specific example we now consider two-flavor mixing between ν_e and ν_μ , and write down the Hamiltonian in the weak interaction basis. It is connected to the mass basis by virtue of the unitary transformation $\nu_\alpha = U_{\alpha i} \nu_i$ of Eq. (22). The squared mass matrix then transforms as UM^2U^\dagger , leading in the weak basis explicitly to

$$M^2 = \frac{\Sigma}{2} + \frac{\delta m^2}{2} \begin{pmatrix} -\cos 2\theta & \sin 2\theta \\ \sin 2\theta & \cos 2\theta \end{pmatrix}, \quad (37)$$

where $\Sigma = m_2^2 + m_1^2$ and $\delta m^2 = m_2^2 - m_1^2$. Including the weak potential then leads to the ‘‘Hamiltonian’’

$$\begin{aligned} \Omega_M &= \frac{\Sigma}{4E} + \frac{\delta m^2}{4E} \begin{pmatrix} -\cos 2\theta & \sin 2\theta \\ \sin 2\theta & \cos 2\theta \end{pmatrix} + \sqrt{2}G_F \begin{pmatrix} n_e - \frac{1}{2}n_n & 0 \\ 0 & -\frac{1}{2}n_n \end{pmatrix} \\ &= \frac{1}{2} \left[\frac{\Sigma}{2E} + \sqrt{2}G_F(n_e - n_n) \right] \\ &+ \frac{1}{2} \left(\sqrt{2}G_F n_e - \frac{\delta m^2}{2E} \cos 2\theta \right) \begin{pmatrix} 1 & 0 \\ 0 & -1 \end{pmatrix} + \frac{1}{2} \sin 2\theta \begin{pmatrix} 0 & 1 \\ 1 & 0 \end{pmatrix} \end{aligned} \quad (38)$$

which governs the oscillations in a medium. The first term which is proportional to the unit matrix produces an irrelevant overall phase so that the medium effect on the oscillations depends only on the electron density n_e , i.e. on the *difference* between the weak potentials for ν_e and ν_μ . Recall that this difference arises from the charged-current piece in the ν_e interaction with the electrons of the medium.

The meaning of this complicated-looking expression becomes more transparent if one determines the ‘‘propagation eigenstates,’’ i.e. the basis where Ω_M is diagonal. In vacuum we have $M^2 = 2E\Omega$ so that in the medium one may define an effective mass matrix by virtue of $M_M^2 = 2E\Omega_M$. The eigenvalues m_M^2 of this matrix are found in the usual way by solving $\det(2E\Omega_M - m_M^2) = 0$. The two roots and their difference are found to be

$$m_M^2 = \frac{1}{2} \left(\Sigma + 2\sqrt{2}G_F(n_e - n_n)E \mp \delta m_M^2 \right), \quad (39)$$

$$\delta m_M^2 = \left[(\delta m^2)^2 + 4EG_F n_e \left(2EG_F n_e - \sqrt{2} \delta m^2 \cos 2\theta \right) \right]^{1/2}.$$

In vacuum where $n_e = n_n = 0$ these expressions reduce to $m_{1,2}^2$ and $\delta m^2 = m_2^2 - m_1^2$. We stress that the in-medium effective squared ‘‘masses’’ should not be literally interpreted as effective masses as they depend on energy; m_M^2 may even become negative. The ‘‘effective masses’’ are simply a way to express the dispersion relation in the medium.

The transformation between the in-medium propagation eigenstates and the weak-interaction eigenstates is effected by a unitary transformation of the form Eq. (22) with the in-medium mixing angle

$$\tan 2\theta_M = \frac{\sin 2\theta}{\cos 2\theta - A} \quad (40)$$

which is equivalent to

$$\sin^2 2\theta_M = \frac{\sin^2 2\theta}{(\cos 2\theta - A)^2 + \sin^2 2\theta}. \quad (41)$$

Here

$$A \equiv \frac{2\sqrt{2}EG_F n_e}{\delta m^2} = 1.52 \times 10^{-7} \frac{Y_e \rho}{\text{g cm}^{-3}} \frac{E}{\text{MeV}} \frac{\text{eV}^2}{\delta m^2}, \quad (42)$$

where Y_e is the electron number per baryon and ρ the mass density.

With these results it is trivial to transcribe the oscillation probability from the previous section to this case,

$$P_M(\nu_e \rightarrow \nu_\mu) = \sin^2 2\theta_M \sin^2 \left(\frac{x \delta m_M^2}{4E} \right). \quad (43)$$

Evidently we have

$$\ell_M = \frac{4\pi E}{\delta m_M^2} = \frac{\sin 2\theta_M}{\sin 2\theta} \ell_{\text{vac}}, \quad (44)$$

for the in-medium oscillation length.

2.2.2 MSW Effect

The mixing angle in matter, $\sin^2 2\theta_M$, is a function of n_e and E . It becomes maximal ($\theta_M = \pi/4$) when $A = A_R = \cos 2\theta$. Here δm_M^2 has a minimum, the oscillation length ℓ_M a maximum. Even if the mixing angle in vacuum is small, on resonance the in-medium mixing is maximal, *independently* of the mixing angle in vacuum.

The most interesting situation arises when a neutrino beam passes through a medium with variable density, the main example being solar neutrinos which are produced at high density in the solar core. Considering the case $m_1^2 \simeq 0$ and θ small, we find for high density ($A \gg A_R$) that $\theta_M \simeq \frac{\pi}{2}$, implying

$$\begin{aligned} \nu_{1M} &\simeq -\nu_\mu, & m_{1M}^2 &\simeq 0, \\ \nu_{2M} &\simeq +\nu_e, & m_{2M}^2 &\simeq A \delta m^2. \end{aligned} \quad (45)$$

On the other hand, for low densities ($A \ll A_R$) we have vacuum mixing ($\theta_M \simeq \theta \ll 1$) so that

$$\begin{aligned} \nu_{1M} &\simeq +\nu_e, & m_{1M}^2 &\simeq 0, \\ \nu_{2M} &\simeq +\nu_\mu, & m_{2M}^2 &\simeq m_2^2. \end{aligned} \quad (46)$$

Therefore, the propagation eigenstate ν_{2M} which at high density is approximately a ν_e turns into a ν_μ at low density, and vice versa. Therefore, if the neutrino is born as a ν_e , and if the density variation is adiabatic so that the neutrino can be thought of being in a propagation eigenstate all along its trajectory, it will emerge as a ν_μ .

In order for this resonant conversion to occur, two conditions must be met. First, the production and detection must occur on opposite sides of a layer with the resonant density. In the Sun, the neutrinos are produced at high density so that we need to require

$$A(\text{place of production}) > A_R = \cos 2\theta. \quad (47)$$

This can be rewritten as a constraint on the neutrino energy,

$$E > E_0 = \frac{\delta m^2 \cos 2\theta}{2\sqrt{2}G_F n_e} = 6.6 \times 10^6 \text{ MeV} \cos 2\theta \frac{\delta m^2 \text{ g cm}^{-3}}{\text{eV}^2 Y_e \rho}. \quad (48)$$

Second, for the neutrino to stay in the state ν_{2m} , the density gradient has to be moderate, i.e. the density variation must be small for several oscillation lengths. This condition can be expressed as $\ell_M^{-1} \gg \nabla \ln n_e$. One often defines the adiabaticity parameter

$$\gamma = \frac{\delta m^2 \sin^2 2\theta}{2E \cos 2\theta} \frac{1}{|\nabla \ln n_e|} \quad (49)$$

so that adiabaticity is achieved for $\gamma \ll 1$. This condition must be met along the entire trajectory. As the oscillation length is longest on resonance when the mixing is maximum, the adiabaticity condition is most restrictive on resonance. In general one finds a triangle in $\sin^2 2\theta$ - δm^2 space where these conditions are fulfilled —see Exercise 2.3.2. In Fig. 4 the triangular contours show the range of masses and mixing angles where the solar ν_e flux is reduced to the measured levels for experiments with different spectral response, i.e. which measure different average neutrino energies.

2.3 Exercises

2.3.1 Polarization vector and neutrino oscillations

Neutrino oscillations are frequently described by a Schrödinger equation of the form

$$i\dot{\Psi} = \Omega\Psi \quad \text{with} \quad \Omega = p + \frac{M^2}{2p}, \quad (50)$$

with p the neutrino momentum, M the mass matrix, and Ψ a column vector with two or more flavors. For two generations, the relation between flavor and mass eigenstates is given by Eq. (22). Instead of the state vectors, however, one can work with the 2×2 density matrix in flavor space which is defined by

$$\rho_{ab} = \Psi_b^* \Psi_a, \quad (51)$$

where the indices a and b run, for example, over ν_e and ν_μ or over 1 and 2 in the mass basis. With the help of the density matrix we can find an intuitive geometric interpretation of oscillation phenomena. In addition, one can treat statistical mixtures of states, i.e. when the neutrinos are not characterized by pure states.

- a) Show that the equation of motion is: $i\dot{\rho} = [\Omega, \rho] = [M^2, \rho]/2p$.
- b) Write the mass matrix in the form $M^2/2p = V_0 - \frac{1}{2}\mathbf{V} \cdot \boldsymbol{\sigma}$ and show, that in the flavor basis

$$V_0 = \frac{m_2^2 + m_1^2}{4p} \text{ and } \mathbf{V} = \frac{2\pi}{\omega_{\text{osc}}} \begin{pmatrix} \sin 2\theta \\ 0 \\ \cos 2\theta \end{pmatrix} \text{ with } \omega_{\text{osc}} = \frac{4\pi p}{m_2^2 - m_1^2}. \quad (52)$$

The vector \mathbf{V} is thus rotated against the 3-axis with the angle 2θ . Has this orientation in the 1–2 plain a physical meaning?

- c) Express the density matrix in terms of a polarization vector in form of $\rho = \frac{1}{2}(1 + \mathbf{P} \cdot \boldsymbol{\sigma})$. Physical interpretation of its components?
- d) Which property of \mathbf{P} characterizes the “purity” of the state, i.e. when does the density matrix describe pure states, when maximally incoherent mixing?
- e) Show that the equation of motion is a precession formula, $\dot{\mathbf{P}} = \mathbf{V} \cdot \mathbf{P}$. Obtain the oscillation probability for an initial ν_e .
- f) The energy of (non-mixed) relativistic neutrinos in a normal medium is $E = p + (m^2/2p) + V_{\text{med}}$. Here V_{med} is given by Eq. (11). What is \mathbf{P} in the medium? What is the mixing angle in the medium?
- g) In a medium consisting of neutrinos (supernova, early universe) one can not distinguish between a test neutrino and a background neutrino, so that oscillations with medium effects are in general nonlinear. What is the advantage of the density matrix formalism in this situation?

2.3.2 MSW Effect in the Sun

The conditions for the MSW effect are given by the Eqs. (48) and (49). Determine the region in $\sin^2 2\theta - \delta m^2$ space, where one expects almost complete flavor inversion, i.e. the MSW triangle. For this purpose, assume that all solar neutrinos are produced with an energy of $E = 1$ MeV and that the density profile of the Sun is approximated by an exponential of the form $n_e = n_c \exp(-r/R_0)$, with a scale height of $R_0 = R_\odot/10.54$ and a density at the center of $n_c = 1.6 \times 10^{26} \text{ cm}^{-3}$.

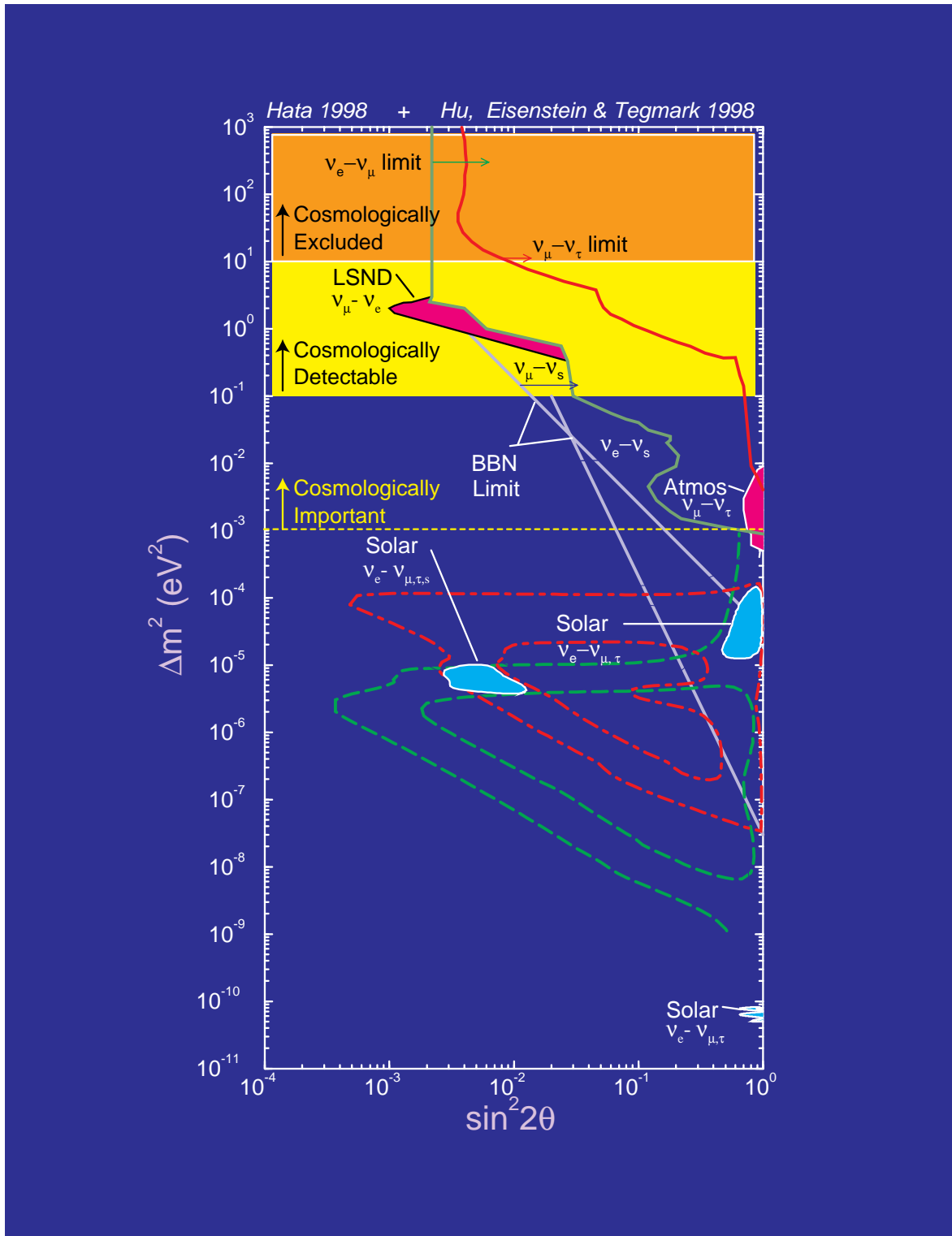


Figure 4: Limits and evidence for neutrino oscillations (Figure courtesy of Max Tegmark).

3 Experimental Oscillation Searches

3.1 Typical Scales

We now turn to a discussion of some experimental strategies for the detection of neutrino oscillations. The most widely used neutrino sources are the Sun, the Earth's atmosphere where neutrinos emerge from cosmic-ray interactions, or man-made devices such as reactors and accelerators. One distinguishes between appearance and disappearance experiments. In the former, one searches for the appearance of another flavor than has been produced in the source, while the latter are only sensitive to a deficit of the original flux.

From Eq. (28) one finds that an experiment with typical neutrino energies E and a distance L between source and detector is sensitive to a minimal value of the mass-squared difference of

$$(\delta m^2)_{\min} \simeq \frac{E}{L}. \quad (53)$$

Therefore, different experiments probe different regions of the mass sector. In Table 3 we give some examples.

Table 3: Characteristics of typical oscillation experiments.

Source	Flavor	E [GeV]	L [km]	$(\delta m^2)_{\min}$ [eV ²]
Atmosphere	$\bar{\nu}_e, \bar{\nu}_\mu$	$10^{-1} \dots 10^2$	$10 \dots 10^4$	10^{-6}
Sun	ν_e	$10^{-3} \dots 10^{-2}$	10^8	10^{-11}
Reactor	$\bar{\nu}_e$	$10^{-4} \dots 10^{-2}$	10^{-1}	10^{-3}
Accelerator	$\nu_e, \bar{\nu}_\mu$	$10^{-1} \dots 1$	10^2	10^{-1}

3.2 Atmospheric neutrino experiments

When cosmic rays, i.e. protons and heavier nuclei interact with the Earth's atmosphere they produce kaons and pions, which in turn decay into muons, electrons and neutrinos. Since the initial state is positively charged one has more neutrinos than anti-neutrinos, but the experiments are insensitive to this effect. On the other hand, the flavor can be very well measured; from the simple production mechanism one expects

$$N(\nu_\mu) : N(\nu_e) = 2 : 1. \quad (54)$$

This ratio depends on the energy of the measured neutrinos since the lifetime of high-energy muons is increased by their Lorentz factor so that they may hit the ground before decaying. One often uses the double ratio

$$R = \frac{(N(\mu)/N(e))_{\text{meas}}}{(N(\mu)/N(e))_{\text{MC}}}, \quad (55)$$

meaning the ratio of the measured flavor ratio divided by the expectation from Monte-Carlo simulations. The double ratio has the advantage that the uncertainty of the overall absolute flux cancels out. The average neutrino energy is found to be $\langle E_\nu \rangle \simeq 0.6$ GeV.

A textbook example of an experiment of this kind is SuperKamiokande (SK) [13], an underground detector consisting of 50 kt of water, surrounded by 11000 photomultipliers. Neutrinos react with the protons and neutrons of the target and produce electrons and muons. These charged particles are identified by their cones of Cherenkov light which are fuzzier for the electrons. Since cosmic rays are distributed almost isotropically and the atmosphere is spherically symmetric, one expects the flux to be the same for down or up-coming neutrinos. However, it was found that up-coming muon neutrinos are significantly suppressed. This up-down asymmetry is shown in Fig. 5. Plotted is the momentum of the

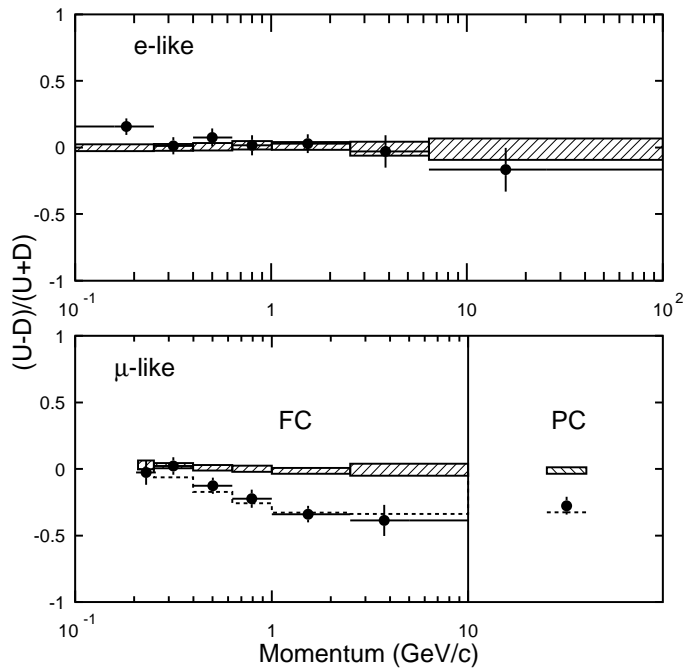


Figure 5: Up-down asymmetry at SK. The hatched region is the expectation without oscillation, the dots the measurements, while the dashed line represents the best-fit oscillation case. (Figure from [13].)

charged leptons against

$$A = \frac{U - D}{U + D}, \quad (56)$$

where U and D are the number of upward and downward going events, i.e. their zenith angle is larger or smaller than about 78° , respectively. The dashed line corresponds to the best-fit mixing parameters of SK, $\delta m^2 = 2.2 \times 10^{-3} \text{ eV}^2$ and $\sin^2 2\theta = 1$. Roughly the same parameters are found by similar experiments, like IMB [14], MACRO [15] or Soudan [16]. For the double ratio R values between 0.4 and 0.7 were found.

Therefore, the ν_μ 's probably oscillate into ν_τ 's. The other possibility, oscillation into sterile neutrinos ν_s is disfavored because the observed rate of the NC process $\nu N \rightarrow \nu \pi^0 X$ is about as expected. Sterile neutrinos by definition do not take part in such reactions. In addition, other properties such as the energy distributions of the final-state charged leptons tend to confirm the ν_μ - ν_τ interpretation.

3.3 Accelerator Experiments

Evidence for oscillations were present before the SuperKamiokande results. The LSND [17] collaboration used a 800 MeV proton beam colliding on a water target so that pions were produced. The π^- were captured in a copper block while the π^+ decayed into $\mu^+\nu_\mu$. These in turn decayed into a positron and two neutrinos. Therefore, one expects the same number of ν_μ , $\bar{\nu}_\mu$ and ν_e , but no $\bar{\nu}_e$. In a scintillation detector 30 m behind the source they looked for $\bar{\nu}_e$ in the reaction $\bar{\nu}_e + p \rightarrow e^+ + n$. The experimental signature is thus the Cherenkov cone from the positron and a photon from the reaction $\gamma + p \rightarrow D + \gamma$ (2.2 MeV).

The LSND collaboration measured an excess of about 40 events above the background. The interpretation as oscillations, however, is controversial because the very similar KARMEN [18] experiment sees no events in about the same parameter range. On the other hand, KARMEN will not be able to exclude the LSND results. The remaining parameter range where a consistent interpretation as oscillations remains possible is shown in Fig. 4, i.e. $\delta m^2 \simeq 1 \text{ eV}^2$ and $\sin^2 2\theta \simeq 10^{-2}$.

3.4 Reactor Experiments

In power reactors, nuclear fission produces $\bar{\nu}_e$ with energies of typically several MeV. These energies are too low to produce a charged mu or tau lepton in the detector so that reactor experiments are always disappearance experiments. The detection reaction is $\bar{\nu}_e + p \rightarrow e^+ + n$.

Thus far, none of the reactor experiment gives evidence for oscillations. However, they have produced very important exclusion areas in the $\sin^2 2\theta$ - δm^2 space. Most importantly,

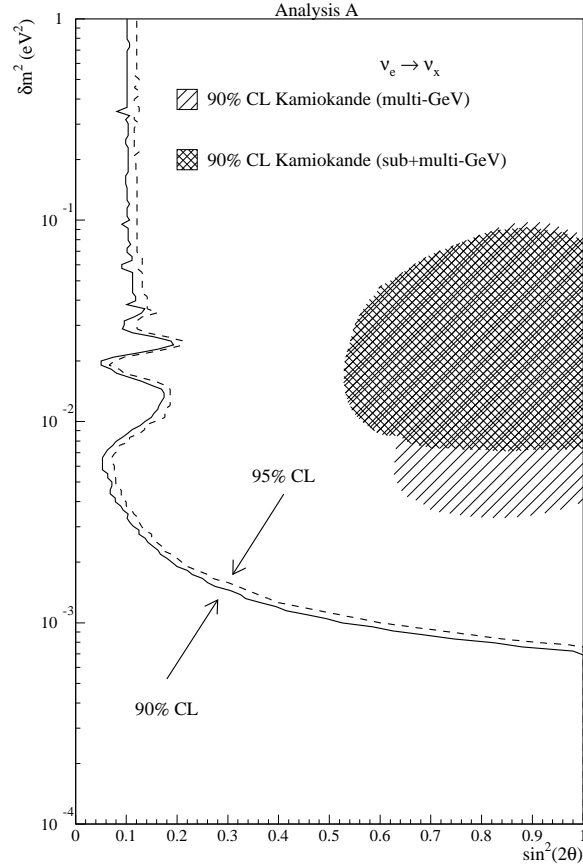


Figure 6: Exclusion plot of the CHOOZ experiment; the area to the right of the lines is excluded. Also shown is the allowed parameter space of Kamiokande. The SK has shifted these values towards lower masses, yet they still lie inside the forbidden area. (Figure from [19].)

the CHOOZ experiment [19] has excluded a large range of mixing parameters (Fig. 6) so that a putative ν_μ - ν_e oscillation interpretation of the SuperKamiokande results is inconsistent with their limits.

3.5 Solar Neutrino Experiments

As discussed in Chapter 1.1, there are six different solar neutrino reactions in the pp chain with six different energy spectra. Different experiments measure neutrinos from different reactions because they have different energy thresholds and different spectral response characteristics. Some of the experiments are Homestake [20] which uses the detection reaction $\nu_e + {}^{37}\text{Cl} \rightarrow {}^{37}\text{Ar} + e^-$ (threshold 814 keV), the gallium experiments GALLEX [21], and SAGE [22] which use $\nu_e + {}^{71}\text{Ga} \rightarrow {}^{71}\text{Ge} + e^-$ (threshold 232 keV) and

(Super)Kamiokande [23, 24] where the elastic scattering on electrons $\nu_e + e^- \rightarrow \nu_e + e^-$ is used (threshold 5 MeV). These experiments have in common that they are deep under the Earth (typically some 1000 m water equivalent) to eliminate backgrounds from cosmic radiation.

Soon after the first experiments were started it was found that one half to two thirds of the neutrino flux was missing. This “solar neutrino problem” is illustrated by Fig. 7 where the measured rates of the chlorine, gallium, and water Cherenkov experiments are juxtaposed with the predictions in the absence of oscillations. It is important to note that the flux suppression is not the same factor in all experiments. Rather, it looks as if there was a distinct spectral dependence of the neutrino deficit.

Total Rates: Standard Model vs. Experiment Bahcall–Pinsonneault 98

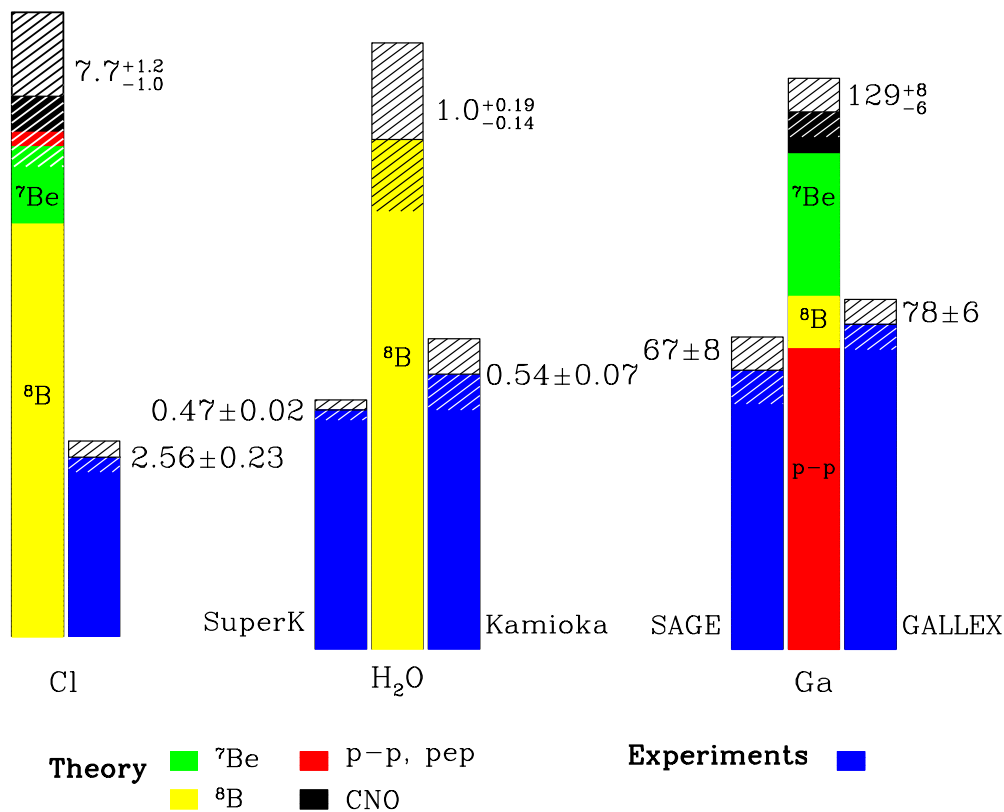


Figure 7: Solar neutrino measurements vs. theoretical flux predictions. (Figure taken from [http://www.sns.ias.edu/~jnb/.](http://www.sns.ias.edu/~jnb/))

In particular, it seems as if the ${}^7\text{Be}$ neutrinos do not reach Earth. Best-fit solutions for SSM flux variations even yield negative ${}^7\text{Be}$ fluxes unless neutrino oscillations are taken into account. Possible non-oscillation explanations seem to be unable to explain this scenario in the light of helioseismology which shows excellent agreement with the SSM. The fact that the nuclear cross sections necessary for the SSM are not known for the relevant (low) energies but have to be extrapolated from higher energy experiments also can not give the measured rates. Temperatures different from the SSM assumption are constrained by the crucial T dependence of the fluxes, namely $\phi_\nu(\text{B}^8) \propto T^{18}$ and $\phi_\nu(\text{Be}^7) \propto T^8$ which do not allow to reduce the beryllium flux by a larger factor than the boron flux.

The solar neutrino measurements can be consistently interpreted in terms of two-flavor oscillations. In contrast to the atmospheric and reactor results, several different solutions exist as shown in Fig. 4. Typical best-fit points are [25]

$$(\delta m^2 \text{ (eV}^2\text{)}, \sin^2 2\theta) = \begin{cases} (5.4 \times 10^{-6}, 6.0 \times 10^{-3}) & \text{SAMSW} \\ (1.8 \times 10^{-5}, 0.76) & \text{LAMSW} \\ (8.0 \times 10^{-11}, 0.75) & \text{VO} \end{cases} \quad (57)$$

Here, SAMSW and LAMSW denote the small-angle and large-angle MSW solution, respectively, while VO refers to vacuum oscillation.

Strategies to decide between these solutions include more precise investigation of the electron energy spectrum (SAMSW/LAMSW) or seasonal variations (VO). A comparison of NC and CC events in the SNO experiment [26] will clarify if the ν_e oscillate into sequential or sterile neutrinos.

3.6 Summary of Experimental Results

With three different masses there can be only two independent δm^2 values. Should all experiments with evidence for oscillations be confirmed then there must be a fourth neutrino, which has to be sterile because LEP measured the number of sequential neutrinos with $m_\nu < 45$ GeV to be 3. The current results can be summarized as

$$(\delta m^2 \text{ (eV}^2\text{)}, \sin^2 2\theta) \simeq \left\{ \begin{array}{ll} (10^{-3}, \gtrsim 0.7) & \text{Atmospheric} \\ (10^{-5}, 10^{-3}) & \text{SAMSW} \\ (10^{-5}, \gtrsim 0.7) & \text{LAMSW} \\ (10^{-10}, \gtrsim 0.7) & \text{VO} \end{array} \right\} \begin{array}{l} \\ \\ \text{Solar} \\ \\ \text{LSND} \end{array} \quad (58)$$

Many authors tend to ignore the LSND results to avoid the seemingly unnatural possibility of a sterile neutrino. On the other hand, if it were found to exist, after all, this would be the most important discovery in neutrino–oscillation physics.

How to choose the masses to get the observed differences is a topic of its own. The most interesting aspect of the mass and mixing scheme is the influence on neutrinoless double beta decay. We refer to [9] for a review of that interesting issue. For later need in the next chapter it suffices to say that if the atmospheric mass scale is interpreted in a hierarchical mass scenario ($\delta m^2 \simeq m^2$) we have one mass eigenstate of about 0.03 eV.

We close this chapter with a few words on future important experiments. For solar physics, besides the SNO experiment, the BOREXINO [27] experiment will measure the crucial ${}^7\text{Be}$ flux to a higher precision than its predecessors. MiniBoone [28] is designed to close the LSND/KARMEN debate and thus confirm or refute the need for a sterile neutrino.

Also planned are so–called long baseline (LBL) accelerator experiments from KEK to Kamioka (K2K, [29]), from Fermilab to Soudan (MINOS, [30]) and from CERN to Gran Sasso (ICARUS, [31]) probing mass ranges down to $\delta m^2 \simeq 10^{-3}$ eV and testing possible CP violation in the neutrino sector. In the years to come, exciting discoveries are to be expected.

4 Neutrinos in Cosmology

4.1 Friedmann Equation and Cosmological Basics

The neutrino plus anti-neutrino density per family in the universe of 113 cm^{-3} is comparable to the photon density of 411 cm^{-3} . Therefore, it is no surprise that neutrinos, especially if they have a non-vanishing mass, may be important in cosmology. To appreciate their cosmological role, we first need to discuss some basic properties of the universe.

On average, the universe is homogeneous and isotropic. Its expansion is governed by the Friedmann equation,

$$H^2 = \frac{8\pi}{3}G_N\rho - \frac{k}{a^2}, \quad (59)$$

where G_N is Newton's constant, ρ the energy density of the universe, and $H = \dot{a}/a$ the expansion parameter with $a(t)$ the cosmic scale factor with the dimension of a length. The present-day value of the expansion parameter is usually called the Hubble constant. It has the value

$$H_0 = h \, 100 \text{ km s}^{-1} \text{ Mpc}^{-1}, \quad (60)$$

where $h = 0.5\text{--}0.8$ is a dimensionless “fudge factor.”

The constant k determines the spatial geometry of the universe which is Euclidean (flat) for $k = 0$, and positively or negatively curved with radius a for $k = \pm 1$, respectively. The universe is spatially closed and will recollapse in the future for $k = +1$. For $k = 0$ or -1 it expands forever and is spatially infinite (open), assuming the simplest topological structure. However, even a flat or negatively curved universe can be closed. An example for a flat closed geometry is a periodic space, i.e. one with the topology of a torus.

Equation (59) must be derived from Einstein's field equations. However, it can also be heuristically derived by a simple Newtonian argument. Since the universe is assumed to be isotropic about every point, we may pick one arbitrary center as the origin of a coordinate system. Next, we consider a test mass m at a distance $R(t) = a(t)r$ from the center, and assume that the homogeneous gravitating mass density is ρ . The total energy of the test mass is conserved and may be written as $E = -\frac{1}{2}Km$. On the other hand,

$$E = T + V = \frac{1}{2}m\dot{R}^2 - \frac{G_N M m}{R}, \quad (61)$$

where $M = R^3\rho 4\pi/3$ is the total mass enclosed by a sphere of radius R . With $K = kr^2$ the Friedmann equation follows. On the basis of a Galileo transformation one can easily show that the Friedmann equation stays the same when transformed to another point, i.e. the expansion looks isotropic from every chosen center.

Some basic characteristics of the expanding universe are easily understood if we study the scaling behavior of the energy density ρ . Nonrelativistic matter (“dust”) is simply

diluted by the expansion, while the total number of “particles” in a co-moving volume, of course, is conserved. Therefore, when matter dominates, we find $\rho \propto a^{-3}$.

For radiation (massless particles), the total number in a comoving volume is also conserved. In addition, we must take the redshift by the cosmic expansion into account. The simplest heuristic derivation is to observe that the cosmic expansion stretches space like a rubber-sheet and thus stretches the periodic pattern defined by a wave phenomenon. Thus the wavelength λ of a particle grows with the cosmic scale factor a , implying that its wave number k and thus its momentum scale as a^{-1} . For radiation we have $\omega = k$ so that the energy of every quantum of radiation decreases inversely with the cosmic scale factor. In summary, the energy density of radiation scales as a^{-4} .

For thermal radiation (blackbody radiation) we may employ the Stefan–Boltzmann law $\rho \propto T^4$ to see that $T \propto a^{-1}$. The temperature of the cosmic microwave background radiation is a direct proxy for the inverse of the cosmic scale factor.

The density in Friedmann’s equation, therefore, decreases at least with a^{-3} so that at late times the curvature term takes over if $k = \pm 1$. Of course, it is frequently assumed that the universe is flat, and certainly the curvature term, if present at all, may only begin to be important today. For $k = -1$, H^2 will never change sign, so the universe expands forever. For $k = +1$, the expansion turns around when $H^2 = 0$, i.e. when $a^{-2} = (8\pi/3)G_N\rho$. Either way, at very early times (large temperature, small scale factor), radiation dominates. Therefore, in the early universe we may neglect the curvature term.

A “critical” or Euclidean universe is characterized by $k = 0$. In this case we have a unique relationship between ρ and H . The density corresponding to the present-day expansion parameter H_0 is called the critical density

$$\rho_c = \frac{3H_0^2}{8\pi G_N} = h^2 1.88 \times 10^{-29} \text{ g cm}^{-3}. \quad (62)$$

The last number is the current value of the critical density, denoted ρ_0 . It translates to about 10^{-5} protons per cm^3 . The density is often expressed as a fraction of the critical density by virtue of $\Omega \equiv \rho/\rho_c$. A value of $\Omega = 1$ corresponds to a flat universe.

The cosmic background radiation, which was first observed in the 1960s, is equivalent to the radiation of a black body with temperature $T = 2.726$ K. Therefore, today’s number density of photons is

$$n_\gamma = 2 \int \frac{d^3\mathbf{p}}{(2\pi)^3} f(\omega) = \frac{2\zeta_3}{\pi^2} T^3 \simeq 411.5 \text{ cm}^{-3}, \quad (63)$$

where $f(\omega) = (e^{\omega/T} - 1)^{-1}$ is the Bose–Einstein distribution function. The energy density of photons (or in general bosons) in the universe is calculated by

$$\rho_\gamma = 2 \int \frac{d^3\mathbf{p}}{(2\pi)^3} \omega f(\omega) = \frac{\pi^2}{15} T^4 \equiv g_B \frac{\pi^2}{30} T^4, \quad (64)$$

where we have introduced the effective number of boson degrees of freedom g_B for later use. Therefore,

$$\Omega_\gamma \equiv \frac{\rho_{\gamma 0}}{\rho_0} \simeq 4.658 \times 10^{-34} \text{ g cm}^{-3} / \rho_0 \simeq 2.480 \times 10^{-5} h^{-2} \quad (65)$$

is the contribution of microwave photons to the critical density.

The fraction of baryons relative to the number of photons in the present-day universe is

$$\eta = \frac{n_B}{n_\gamma} = \eta_{10} \times 10^{-10} \simeq 3 \times 10^{-10}, \quad (66)$$

so that the contribution of baryons to the critical density is merely

$$\Omega_B \equiv \frac{\rho_{B0}}{\rho_0} = \frac{\eta \langle E_B \rangle n_\gamma}{\rho_0} = \frac{\eta m_p n_\gamma}{\rho_0} \simeq 3.6 \times 10^{-3} h^{-2} \eta_{10} \simeq 0.01 h^{-2}, \quad (67)$$

where we took the proton mass as an average baryonic energy.

4.2 Radiation Epoch

In the hot early universe, neutrinos should have been in thermal equilibrium so that one expects a cosmological neutrino sea in analogy to the cosmic microwave background. The number density of one massless thermal neutrino generation is

$$n_{\nu\bar{\nu}} = 2 \int \frac{d^3\mathbf{p}}{(2\pi)^3} f(\omega) = \frac{3\zeta_3}{2\pi^2} T^3, \quad (68)$$

where we have to use the Fermi–Dirac distribution $f(\omega) = (e^{\omega/T} + 1)^{-1}$ for fermions with a vanishing chemical potential. Equation (68) counts two internal degrees of freedom, i.e. it counts left-handed (interacting) neutrinos and (right-handed) anti-neutrinos for a given family. The energy density is

$$\rho_{\nu\bar{\nu}} = g_F \int \frac{d^3\mathbf{p}}{(2\pi)^3} \omega f(\omega) = g_F \frac{7}{8} \frac{\pi^2}{30} T^4 \quad (69)$$

with the effective number of fermion degrees of freedom g_F . The effective number of thermal degrees of freedom is defined by

$$g_* = \sum_{j=\text{bosons}} g_j + \frac{7}{8} \sum_{j=\text{fermions}} g_j, \quad (70)$$

so that the total energy density in radiation is

$$\rho_{\text{rad}} = g_* \frac{\pi^2}{30} T^4. \quad (71)$$

Another important quantity is the entropy density in radiation $S = (p + \rho)/T$. Since for a relativistic gas $p = \rho/3$ we have

$$S = g_* \frac{2\pi^2}{45} T^3. \quad (72)$$

The energy and entropy densities are simply functions of the temperature and of the particle degrees of freedom that are thermally excited at that temperature.

To get a feeling for g_* , we consider some characteristic temperatures. At $T < 100$ MeV, below the QCD phase transition, there are photons, e^\pm , and three flavors of (anti)neutrinos, giving $g_* = 2 + 7/8 \times 10 = 43/4 = 10.75$. At $T = 300$ MeV, significantly above the QCD phase transition, in addition muons (4 fermionic degrees of freedom), eight gluons (2×8 bosonic degrees of freedom) and up, down, and strange quarks ($3 \times 4 \times 3$ fermionic degrees of freedom, counting 3 color degrees of freedom each) were present, resulting in $g_* = 18 + 7/8 \times 44 = 113/2 = 56.5$. The number of degrees of freedom drops dramatically around the QCD phase transition when quarks and gluons condense to confined states of mesons and baryons.

The Friedmann equation for the radiation epoch in the early universe can be written in the form

$$H^2 = \frac{4\pi^3}{45} G_N g_* T^4. \quad (73)$$

We can now calculate a relationship between cosmic age and temperature in the radiation epoch. We use $\rho = \rho_0 (R_0/R)^4 \equiv bR^{-4}$ and $H^2 = 8\pi/3 G_N b R^{-4}$ which leads to

$$\dot{R}(t) = \left(\frac{8\pi}{3} G_N b \right)^{1/2} \frac{1}{R} \quad (74)$$

and thus to

$$R(t) = \left(\frac{32\pi}{3} G_N b \right)^{1/4} t^{1/2}. \quad (75)$$

With Eq. (71) for $\rho(T)$ we find

$$T = \left(\frac{45}{16\pi^3 G_N g_*} \right)^{1/4} t^{-1/2} = g_*^{-1/4} 1.56 \text{ MeV} \left(\frac{1 \text{ s}}{t} \right)^{1/2}. \quad (76)$$

Therefore, the universe had a temperature of about 1 MeV when it was about 1 s old.

4.3 Present–Day Neutrino Density

When neutrinos and photons are in thermal equilibrium in the early universe, they are both characterized by the same temperature. However, the neutrino temperature today is thought to be lower than that of the cosmic microwave background. The reason for the difference is that when the temperature has fallen below the electron mass m_e ($t \simeq 10$ s)

the annihilation of electrons and positrons heats the photon gas by virtue of $e^+e^- \rightarrow 2\gamma$. As we will see later, neutrinos have already decoupled at that time so that the rate for $e^+e^- \rightarrow \nu\bar{\nu}$ is too slow to be of importance.

The electron–positron–photon plasma is so tightly coupled that one may assume that it is always close to thermal equilibrium throughout the annihilation process, i.e. the disappearance of the e^\pm pairs is an adiabatic process. Therefore, the entropy of the e^\pm gas will go over to the photons. If we denote the photon temperature before this process as T_1 and afterward as T_2 , and if the value of g_* for the coupled species before and after annihilation is $g_{1,2}$, respectively, entropy conservation implies

$$g_1 T_1^3 = g_2 T_2^3. \quad (77)$$

Before annihilation, the participating species are e^\pm and photons so that $g_* = 2 + 4 \times 7/8 = 11/2$, while afterward we have only photons with $g_* = 2$. Before annihilation, we have $T_\nu = T_\gamma$ so that the ratio T_2/T_1 can be interpreted as T_γ/T_ν after annihilation. Therefore, we find the famous result

$$T_\nu = \left(\frac{4}{11}\right)^{1/3} T_\gamma. \quad (78)$$

Thus, the present-day temperature of the neutrino background is predicted to be $T_\nu \simeq 1.946 \text{ K} \simeq 1.678 \times 10^{-4} \text{ eV}$. Naturally, its direct detection is an impossible task.

The number density of one neutrino family is given by Eq. (68). Inserting the above numbers yields

$$n_{\nu\bar{\nu}} \simeq 337.5 \text{ cm}^{-3} \quad (79)$$

for all three generations. If all neutrinos are relativistic today, all three families contribute

$$\rho_{\nu\bar{\nu}} = \frac{7}{8} \left(\frac{4}{11}\right)^{4/3} \frac{3g_\nu}{g_\gamma} \rho_\gamma \simeq 3.174 \times 10^{-34} \text{ g cm}^{-3} \quad (80)$$

to the cosmic energy density.

We have assumed that the neutrinos are relativistic, which is the case when their mass is smaller than their average energy

$$\langle E_\nu \rangle = \frac{\rho_{\nu\bar{\nu}}}{n_{\nu\bar{\nu}}} \simeq 3 T_\nu \simeq 5 \times 10^{-4} \text{ eV}. \quad (81)$$

If the indications for neutrino oscillations discussed in the previous section are correct, at least one of the mass eigenstates exceeds around 0.03 eV and thus is not relativistic today.

But even if m_ν is bigger than $5 \times 10^{-4} \text{ eV}$, the number density is still given by Eq. (79) since at the point of e^\pm annihilation the neutrinos were relativistic. The energy density

today, though, changes for one nonrelativistic flavor to $\rho_{\nu\bar{\nu}} = n_{\nu\bar{\nu}}m_\nu$. The contribution to the critical density today is then $\Omega_{\nu\bar{\nu}} \equiv \rho_{\nu\bar{\nu}}/\rho_c$ or

$$\Omega_{\nu\bar{\nu}}h^2 \simeq \sum_{\text{flavors}} \frac{m_\nu}{94 \text{ eV}}. \quad (82)$$

We may use this result to derive the famous cosmological limit on the neutrino masses. It turns out that the lower limit on the age of the universe indicated by the age of globular clusters implies something like $\Omega h^2 \lesssim 0.4$. Since $\Omega_{\nu\bar{\nu}} < \Omega$ we have

$$\sum_{\text{flavors}} m_\nu \lesssim 37 \text{ eV}. \quad (83)$$

If the experimental indications for neutrino oscillations are correct, the mass differences are very small. Therefore, a neutrino mass in the neighborhood of this limit would require that all flavors have nearly degenerate masses, implying that we may divide this limit by the number of flavors to obtain a limit on the individual masses. Therefore,

$$m_\nu \lesssim 12 \text{ eV} \quad (84)$$

applies to all sequential neutrinos.

If the current indications for oscillations from the atmospheric neutrino anomaly are correct so that one mass eigenstate exceeds about 0.03 eV we find that $\Omega_{\nu\bar{\nu}}h^2 \gtrsim 3 \times 10^{-4}$ or, with $h \lesssim 0.8$, we have $\Omega_{\nu\bar{\nu}} \gtrsim 5 \times 10^{-4}$, not much less than the luminous matter of the universe.

One may wonder if any of these results change if neutrinos are Dirac particles so that there are actually 4 degrees of freedom per flavor. However, the sterile (right-handed) components will not be thermally excited in the relevant epochs of the early universe because they are too weakly coupled if the masses are as small as indicated by the cosmological limit. It is important to realize that g_* is the effective number of *thermally excited* degrees of freedom, which does not necessarily include all existing particles. For example, the massless gravitons are another species which are not thermally excited anywhere near the QCD or e^\pm annihilation epochs so that they, too, have not appeared in our particle counting for g_* .

4.4 Big Bang Nucleosynthesis

How do we know that the cosmological neutrino background actually exists? After all, its direct detection is an impossible task with present-day experimental means. However, the cosmic neutrinos manifest themselves directly in the process of forming the lightest nuclei in the early universe so that Big Bang Nucleosynthesis (BBN) yields compelling evidence for the reality of the “cosmic neutrino sea.”

All of the deuterium and most of the helium in the present-day universe can not have been produced in stars, so that it must have been produced shortly after the Big Bang. The process of primordial nucleosynthesis explains today's abundance of several light elements, notably ${}^4\text{He}$, D, ${}^3\text{He}$ and ${}^7\text{Li}$. Perhaps the most important quantity is the mass fraction Y_p of primordial ${}^4\text{He}$, which is observationally inferred to be

$$Y_p \equiv \frac{M_{\text{He}}}{M_{\text{H}} + M_{\text{He}}} \simeq 0.24. \quad (85)$$

The abundances of the other elements are very much smaller; for example $n_{\text{D}+{}^3\text{He}}/n_{\text{H}} \simeq 10^{-5}$, $n_{\text{Li}}/n_{\text{H}} \simeq 10^{-10}$.

In a thermal plasma, all nuclei should be present with their thermal equilibrium abundance given by nuclear statistical equilibrium (NSE). The abundance of nuclei with atomic number A , nuclear charge Z , binding energy B_A , and a statistical factor g_A is [3]

$$n_A = g_A A^{3/2} 2^{-A} \left(\frac{2\pi}{m_N T} \right)^{\frac{3(A-1)}{2}} n_p^Z n_N^{A-Z} \exp B_A/T. \quad (86)$$

For example, $g_A = 2$ for ${}^3\text{He}$ which has total spin $1/2$.

At high temperatures, there are very few nuclei because the dissociated state is preferred. The early universe is a “high-entropy environment” because there are about 10^{10} thermal photons per baryon. Therefore, the dissociated state is favored until very late when the temperature is significantly below the typical nuclear binding energies. The main idea behind BBN is that nuclei stayed dissociated until very late so that they appear in appreciable numbers only at a time when the reactions forming and dissociating them begin to freeze out of thermal equilibrium. Therefore, hardly any nuclei heavier than helium form at all —otherwise one might have expected that most of the matter appears in the form of iron, the most tightly bound nucleus.

Nuclei are produced from protons and neutrons which, at high temperatures, are in thermal equilibrium by β -processes of the form

$$\bar{\nu}_e + p \leftrightarrow e^+ + n, \quad \nu_e + n \leftrightarrow e^- + p, \quad n \leftrightarrow p + e^- + \bar{\nu}_e. \quad (87)$$

These processes “freeze out” when they become slow relative to the expansion rate of the universe. By dimensional analysis the reaction rates are of the form

$$\Gamma \propto G_F^2 T^5. \quad (88)$$

The other characteristic time scale is defined by the Hubble parameter H which has the form

$$H \propto \frac{1}{m_{\text{Pl}}} T^2, \quad (89)$$

where we write Newton's constant as the inverse of the Planck mass squared. Therefore the expansion of the universe was too fast for the rates when $H > \Gamma$, which leads to a freeze-out temperature of

$$T_F \simeq 0.8 \text{ MeV}. \quad (90)$$

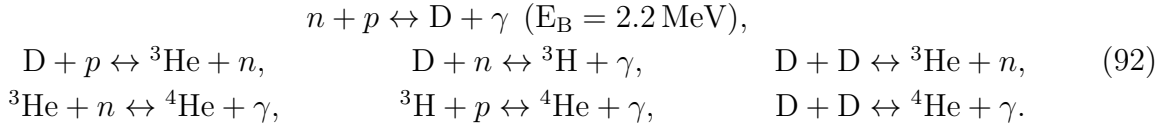
At lower temperatures (later times) weak processes and thus neutrinos are no longer in equilibrium.

Before the weak reactions became ineffective, the ratio of protons and neutrons was given thermal equilibrium as

$$\frac{n_n}{n_p} = \exp\left(\frac{-Q}{T}\right), \quad (91)$$

where $Q = m_n - m_p = 1.293 \text{ MeV}$. When $T < T_F$ (after about 1 s), the ratio changes only by neutron free decays with a neutron lifetime of $\tau_n \simeq 887 \text{ s}$, i.e. it decreases as $\exp(-t/\tau_n)$.

At T_F when the weak interactions froze out, the neutron/proton ratio was about 1/6. After the temperature fell below about 0.1 MeV at a cosmic age of about 3 min, BBN began in earnest. Some important reactions involving the first few steps are



Most of the reactions end in ${}^4\text{He}$. Heavier elements do not efficiently form because they have too large Coloumb barriers. Moreover, there are bottlenecks in the reaction network because there are no stable nuclei with $A = 5$ or $A = 8$.

At higher temperatures the deuteron produced in the first reaction was immediately dissociated by photons, which have an average energy of $\langle E_\gamma \rangle = \rho_\gamma/n_\gamma \simeq 2.70 T$. These dissociating photons were available in great number since the baryon/photon ratio $\eta = \eta_{10} 10^{-10}$ is very small. When $\eta \exp(E_B/T) \simeq 1$, deuterons were produced in sufficient numbers. This requirement gives a temperature of about 0.1 MeV and thus defines the beginning of BBN.

When all remaining neutrons had disappeared in ${}^4\text{He}$, we have $M_{\text{He}} = n_n 2m_N$ and $M_{\text{H}} = (n_p - n_n)m_N$, which leads to a BBN prediction for the helium mass fraction of

$$Y_p = \frac{2n_n}{n_p + n_n}. \quad (93)$$

Since BBN stopped about three minutes after the weak reactions Eq. (87) froze out, we get $n_n/n_p \simeq 1/7$ and thus $Y_p \simeq 0.24$ in agreement with the observations.

All of our estimates depend on the freeze-out temperature T_F . It would be higher if H were larger than implied by the standard value for g_* . A larger T_F implies an increased

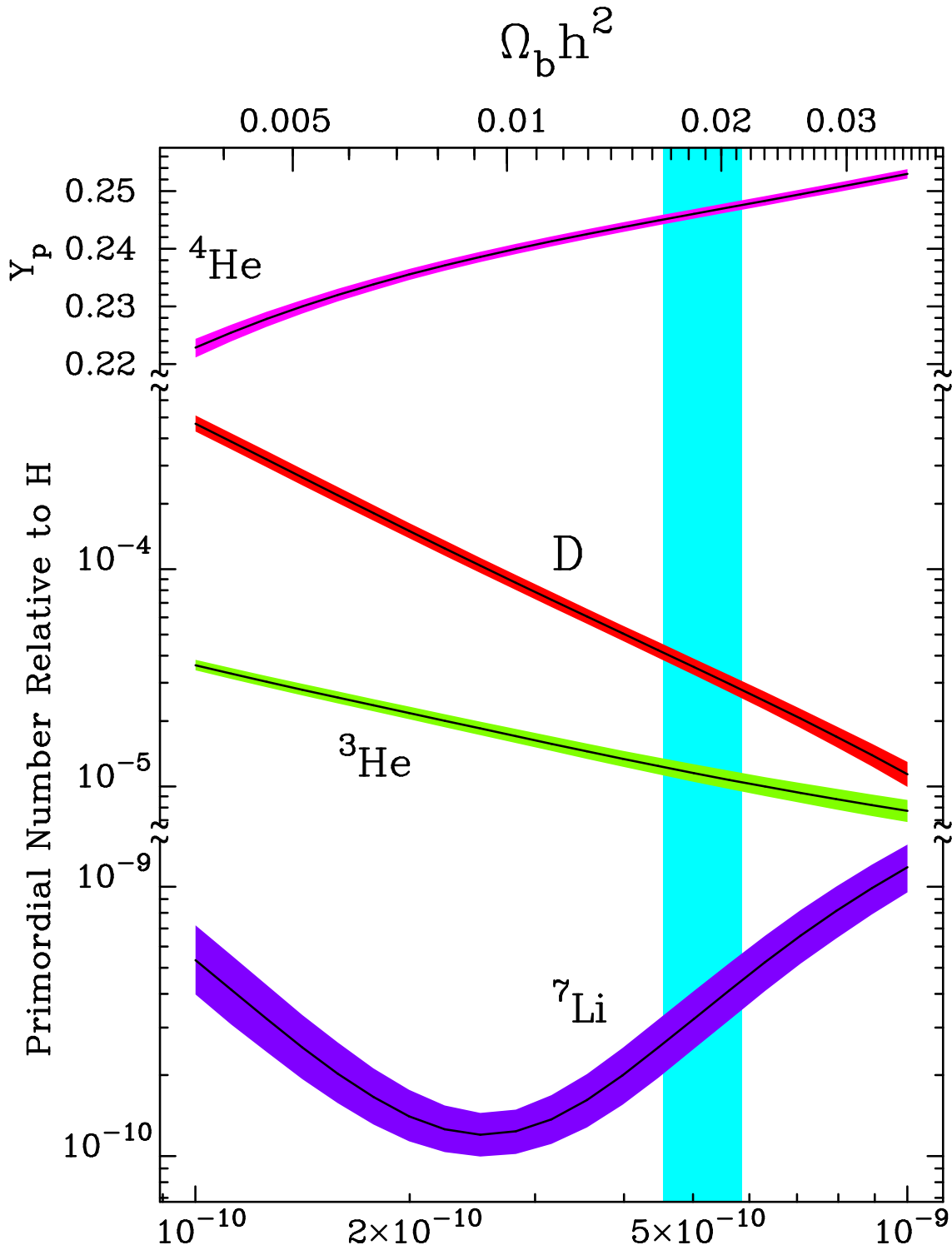


Figure 8: Typical BBN predictions (solid line) for Y_p , D , ${}^3\text{He}$ and ${}^7\text{Li}$ relative to H with 2σ theoretical uncertainty. The vertical band represents a recent measurement of the deuterium abundance [32]. (Figure from [33].)

n_n/n_p and thus an increase of Y_p . Since H is proportional to $g_*^{1/2}$ we find that additional neutrino families would lead to a higher Y_p . This argument was used to constrain the number of neutrino flavors before the famous LEP experiment at CERN. In [33] one finds that for $Y_p = 0.246 \pm 0.0014$ the number of neutrino species is limited by $N_\nu < 3.20$ at 95% C.L.

The theoretical dependence of the light element abundances on η is shown in Fig. 8, assuming the standard number of neutrino families $N_\nu = 3$. The BBN predictions explain abundances consistently over a range of 10 orders of magnitude. Therefore, at the present time it appears that BBN is a consistent theory. It certainly requires the presence of thermal neutrinos and thus can be taken as compelling evidence for the reality of the cosmic neutrino sea.

4.5 Neutrinos as Dark Matter

The experimental evidence for neutrino oscillations is now so compelling that the reality of non-vanishing neutrino masses must be taken as a serious working hypothesis. However, neutrinos are not a good candidate for the ubiquitous dark matter (DM) which dominates the dynamics of the universe.

One of the most conspicuous dark matter problems is that of the flat galactic rotation curves, implying that the dynamical mass of the galaxy is dominated by some non-luminous component. Assuming that this mass density consist of neutrinos, their maximum phase-space density implied by the Pauli exclusion principle is

$$n_{\max} \equiv \frac{p_{\max}^3}{3\pi^2}. \quad (94)$$

Here, $p_{\max} = m_\nu v_{\max}$ is the maximum momentum of a neutrino bound to the galaxy with v_{\max} the escape velocity of order 500 km s^{-1} . Since $\rho_{\nu\text{DM}} = n_\nu m_\nu$ we obtain a *lower* limit for m_ν . For typical spiral galaxies one finds $m_\nu > 20\text{--}30 \text{ eV}$, and much larger values for dwarf galaxies which are dominated by dark matter. This limit, known as the Tremaine–Gunn bound [34], at least nominally excludes neutrinos as the main component of galactic dark matter.

Even more severe problems arise from arguments about cosmic structure formation. The universe is thought to have started from an almost homogeneous early phase with low-amplitude primordial density fluctuations which must have been produced by some physical process; one favored scenario involves the generation of the primordial fluctuation spectrum during an early phase of exponential expansion (inflation). The density contrast of these primordial fluctuations increases by the action of gravity since any region with more mass than its surroundings will attract more mass, at the expense of lower-density

regions. This gravitational instability mechanism can beautifully account for the observed structure in the matter distribution.

However, weakly interacting particles become collisionless early and thus can travel large distances undisturbed. In this way they will wash out the primordial density fields by their “free streaming” or “collisionless phase mixing” and thus remove the seeds for structure formation up to a certain scale. The smaller the mass, the later these particles will become nonrelativistic, the further they travel, and thus the larger the scales below which the primordial field of density fluctuations has been erased. If all scales up to those which later correspond to galaxies have been erased, the particles are called “hot dark matter” while otherwise they are referred to as “cold dark matter.” The division line between the two notions corresponds to a particle mass in the few keV range.

Since hot dark matter can not account for the observed structures within the standard model of structure formation, they are strongly disfavored, except perhaps as a subdominant component in a hot plus cold dark matter scenario. It is quite surprising that oscillation experiments have established neutrino masses, but that neutrinos nevertheless are no good dark matter candidates.

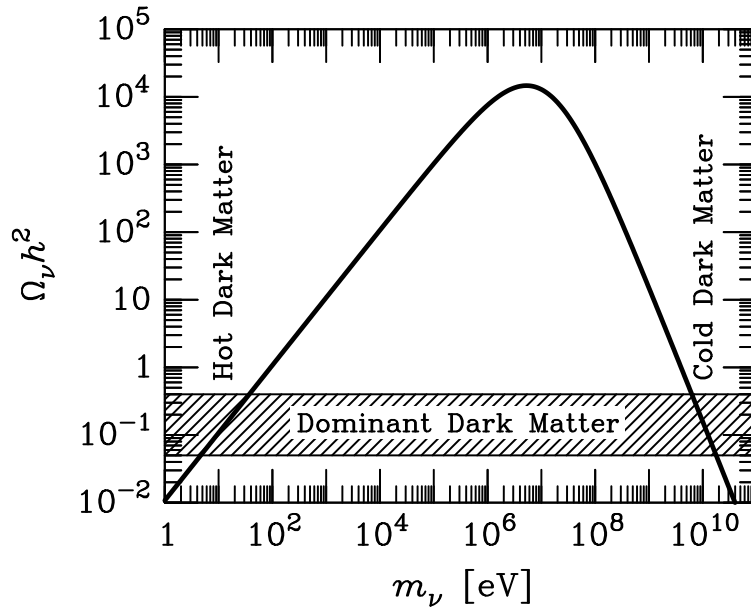


Figure 9: Contribution of massive neutrinos to Ω .

It is widely believed that the dark matter consists of some new, heavy, neutrino-like particles generically referred to as WIMPs (weakly interacting massive particles). One may think that such a cold dark matter particle would vastly overclose the universe since the cosmological mass limit on neutrinos requires a mass less than a few ten eV. However, if

the weakly interacting particles are heavier than a few MeV, the weak–interaction freeze–out happens when the temperature has fallen below their mass. Therefore, their number density is decimated by annihilations, i.e. their thermal equilibrium density is suppressed by a Boltzmann factor $e^{-m/T}$ until the annihilation rate becomes too slow to keep up with the cosmic expansion. Therefore, as a function of the assumed mass of a weakly interacting particle one obtains a cosmic density contribution schematically shown in Fig. 9. This “Lee–Weinberg curve” turns over for large neutrino masses so that there is a second solution at masses of a few or a few ten GeV where neutrinos could be the dark matter, and then of the cold variety.

Of course, none of the sequential neutrinos can play this role because their masses are too small. Even if we ignore the oscillation data, the direct kinematical mass limits are so restrictive (about 18 MeV for ν_τ , the worst case) that standard neutrinos can not play the role of cold dark matter. However, in popular extensions of the standard model the existence of the requisite particles is quite plausible. Notably the theory of supersymmetry provides an ideal candidate in the guise of the “neutralino,” a neutral spin–1/2 Majorana fermion. From a cosmological perspective, these neutralinos are virtually identical with a heavy Majorana neutrino. Even if the standard neutrinos are not the dark matter of the universe, it still looks like weakly interacting particles make up the bulk of the mass in our universe.

5 Conclusions

The question if neutrinos, the most elusive of all elementary particles, have nonvanishing masses has come very close to a conclusion over the past few years. For a long time it had been suspected that the solar neutrino problem is solved by neutrino oscillations and thus by neutrino masses. However, it took the spectacular up–down asymmetry of the atmospheric neutrino flux observed by the SuperKamiokande detector to convince most of the sceptics that neutrino oscillations are real. It is remarkable that natural neutrino sources, the Sun and the upper atmosphere, play a central role at putting together the pieces of the jigsaw puzzle of the leptonic CKM matrix.

As we learn more about the neutrino masses and mixing parameters, there is a certain sense that neutrino masses are too small to be of great cosmological importance. To be sure, it is still possible that the global neutrino mass scale is much larger than their mass differences. In such a degenerate scheme, neutrinos could still play a role as a subdominant dark matter component in hot plus cold dark matter cosmologies. It is also still possible that sterile neutrinos exist. If this hypothesis were verified, neutrinos would be assured of an important role for cosmic structure formation and might modify the standard theory of Big Bang nucleosynthesis.

One should take note that neutrino astrophysics is a field much broader than the question of the neutrino mixing matrix. Once the mixing parameters and masses have been settled, one has greater confidence in one's treatment of astrophysical phenomena where neutrino masses and oscillations are potentially important such as supernovae or gamma-ray bursts, or in the use of neutrinos as a new form of radiation to do astronomy with. Neutrino physics and astrophysics will keep us busy for some time to come!

A Useful Tables

A.1 Integrals

The following integrals frequently appear in the context of calculations involving particle reactions in thermal media, where ζ refers to the Riemann zeta function.

Table 1: Thermal integrals.

	Maxwell–Boltzmann	Fermi–Dirac	Bose–Einstein
	$\int_0^\infty \frac{x^n}{e^x} dx$	$\int_0^\infty \frac{x^n}{e^x + 1} dx$	$\int_0^\infty \frac{x^n}{e^x - 1} dx$
$n = 2$	2	$\frac{3}{2}\zeta_3 \simeq 1.8031$	$2\zeta_3 \simeq 2.40411$
$n = 3$	6	$\frac{7\pi^4}{120} \simeq 5.6822$	$\frac{\pi^4}{15} \simeq 6.4939$

A.2 Conversion of Units

We always use natural units where $\hbar = c = k_B = 1$. In order to convert between different measures of length, time, mass, or energy one may use the following table. For example, $1 \text{ cm}^{-1} = 2.998 \times 10^{10} \text{ s}^{-1}$. The atomic mass unit is denoted by amu.

Table 2: Conversion factors for natural units.

	s^{-1}	cm^{-1}	K	eV	amu	erg	g
s^{-1}	1	0.334×10^{-10}	0.764×10^{-11}	0.658×10^{-15}	0.707×10^{-24}	1.055×10^{-27}	1.173×10^{-48}
cm^{-1}	2.998×10^{10}	1	0.229	1.973×10^{-5}	2.118×10^{-14}	3.161×10^{-17}	0.352×10^{-37}
K	1.310×10^{11}	4.369	1	0.862×10^{-4}	0.962×10^{-13}	1.381×10^{-16}	1.537×10^{-37}
eV	1.519×10^{15}	0.507×10^5	1.160×10^4	1	1.074×10^{-9}	1.602×10^{-12}	1.783×10^{-33}
amu	1.415×10^{24}	0.472×10^{14}	1.081×10^{13}	0.931×10^9	1	1.492×10^{-3}	1.661×10^{-24}
erg	0.948×10^{27}	0.316×10^{17}	0.724×10^{16}	0.624×10^{12}	0.670×10^3	1	1.113×10^{-21}
g	0.852×10^{48}	2.843×10^{37}	0.651×10^{37}	0.561×10^{33}	0.602×10^{24}	0.899×10^{21}	1

References

- [1] N. Schmitz, *Neutrino-physik* (Teubner Studienbücher, 1997).
- [2] G. Raffelt, *Stars as Laboratories for Fundamental Physics* (Chicago Press, 1996).
- [3] E. W. Kolb, M.S. Turner, *The Early Universe* (Addison Wesley, 1993).
- [4] H.V. Klapdor-Kleingrothaus, K. Zuber, *Teilchenastrophysik* (Teubner Studienbücher, 1997).
- [5] L. Bergström, A. Goobar, *Cosmology and Particle Astrophysics* (Wiley, 1999).
- [6] K. Zuber, *Phys. Rep.* **305** (1998) 295.
- [7] G. Raffelt, hep-ph/9902271.
- [8] G. Raffelt, *Annu. Rev. Nucl. Part. Sci.* **49** (1999) in press.
- [9] W. G. S. M. Bilenky, C. Giunti, *Prog. Part. Nucl. Phys.* **43** (1999) 1.
- [10] D. D. Clayton, *Principles of Stellar Evolution and Nucleosynthesis* (University of Chicago Press, 1968).
- [11] R. Kippenhahn, A. Weigert, *Stellar Structure and Evolution* (Springer, 1990).
- [12] J. N. Bahcall, S. Basu, M. H. Pinsonneault, *Phys. Lett. B* **433** (1998) 1.
- [13] (SuperKamiokande collaboration) Y. Fukuda, *Phys. Rev. Lett.* **81** (1998) 1562.
- [14] (IMB collaboration) R. Becker-Szendy *et al.*, *Nucl. Phys. B Proc. Suppl* **83** (1995) 331.
- [15] (MACRO collaboration) M. Ambrosio *et al.*, *Phys. Lett. B* **434** (1998) 451.
- [16] (Soudan collaboration) W. W. M. Allison *et al.*, *Phys. Lett. B* **449** (1999) 137.
- [17] (LSND collaboration) C. Athanassopoulos *et al.*, *Phys. Rev. C* **58** (1998) 2489.
- [18] (KARMEN collaboration) B. Zeitnitz *et al.*, *Prog. Nucl. Part. Phys.* **40** (1998) 169.
- [19] (CHOOZ collaboration) M. Apollonio *et al.*, *Phys. Lett. B* **420** (1998) 397.
- [20] (Homestake Kollaboration) R. Davis *et al.*, *Nucl. Phys. (Proc. Suppl.)* **B 48** (1996) 284.

- [21] (GALLEX collaboration) W. Hampel *et al.*, *Phys. Lett.* **B 388** (1996) 364.
- [22] (SAGE Kollaboration) V. Gavrin in *Proceedings of the XVIII International Conference on Neutrino Physics and Astrophysics*, Takayama, Japan, Juni 1998.
- [23] (SuperKamiokande collaboration) *et al.*, *Phys. Rev. Lett.* **81** (1998) 1158.
- [24] (Kamiokande collaboration) Y. Fukuda *et al.*, *Phys. Rev. Lett.* **77** (1996) 1683.
- [25] J. N. Bahcall, P. I. Krastev, A. Y. Smirnov, *Phys. Rev.* **D 58** (1998) 096016.
- [26] (SNO collaboration) J. Boger *et al.*, nucl-ex/9910016.
- [27] L. Oberauer, *Nucl. Phys. B (Proc. Suppl.)* **77** (1999) 48.
- [28] E. Church *et al.* nucl-ex/9706011.
- [29] K. Nishikawa, *Nucl. Phys. (Proc. Suppl.)* **B 77** (1999) 198.
- [30] S. Wojcicki, *Nucl. Phys. (Proc. Suppl.)* **B 77** (1999) 182.
- [31] C. Rubbia, *Nucl. Phys. (Proc. Suppl.)* **B 48** (1996) 172.
- [32] S. Burles, D. Tytler, *Astrophys. J.* **499** (1998) 699,
ibid. **507** 732.
- [33] S. Burles, *et al.*, *Phys. Rev. Lett.* **82** (1999) 4176, in press.
- [34] S. Tremaine, J. Gunn, *Phys. Rev. Lett.* **42** (1979) 407.